β-1,3-GLUCANASE10 regulates tomato development and disease resistance by modulating callose deposition

Yangang Pei[1#], Qihan Xue[1#], Zehong Zhang[1], Peng Shu[1], Heng Deng[1], Mondher Bouzayen[2], Yiguo Hong[3,4,5], Mingchun Liu[1*s]

[1]Key Laboratory of Bio-Resource and Eco-Environment of Ministry of Education, College of Life Sciences, Sichuan University, Chengdu, 610065, Sichuan, China

[2]Laboratoire de Recherche en Sciences Végétales—Génomique et Biotechnologie des Fruits—UMR5546, Université de Toulouse, CNRS, UPS, Toulouse-INP, Toulouse, France

[3]School of Life Sciences, University of Warwick, Warwick CV4 7AL, UK

[4]School of Science and the Environment, University of Worcester, Worcester WR2 6AJ, UK

[5]Research Centre for Plant RNA Signaling, College of Life and Environmental Sciences, Hangzhou Normal University, Hangzhou 311121, China

[#] These authors contributed equally

[*] Corresponding author (mcliu@scu.edu.cn)

Short title: SlBG10 regulates multiple developmental processes

The author responsible for distribution of materials integral to the findings presented in this article in accordance with the policy described in the Instructions for Authors (https://academic.oup.com/plphys/pages/General-Instructions) is: Mingchun Liu (mcliu@scu.edu.cn).

One-sentence summary: The β-1,3-glucanase SlBG10 acts as a key regulator in fruit set, early seed development, and fruit quality maintenance by modulating callose deposition in tomato.

Abstract

β-1,3-Glucanases are considered key regulators responsible for the degradation of callose in plants, yet little is known about the role and mode of action of their encoding genes in tomato (*Solanum lycopersicum*). In the present study, we identified the β-1,3-glucanase encoding gene *β-1,3-GLUCANASE10* (*SlBG10*) and revealed its regulation in tomato pollen and fruit development, seed production, and disease resistance by modulating callose deposition. Compared to wild-type or *SlBG10* overexpressing (*SlBG10*-OE) lines, knockout of *SlBG10* caused pollen arrest and failure to set fruit with reduced male rather than female fecundity. Further analyses showed that *SlBG10*-knockout promoted callose deposition in anther at the tetrad-to-microspore stages, resulting in pollen abortion and male sterility. Moreover, loss-of-function *SlBG10* delayed degradation of endosperm cell wall calloses during cellularization and impeded early seed development. We also uncovered that *Botrytis cinerea* infection induces *SlBG10* expression in wild-type tomato, and the knockout lines showed increased callose accumulation in fruit pericarps, reduced susceptibility to *B. cinerea* and enhanced antioxidant capacity to maintain tomato fruit quality. However, expression of genes encoding cell wall hydrolases decreased in *SlBG10*-knockout tomatoes and thus led to an increase in pericarp epidermal thickness, enhancement in fruit firmness, reduction of fruit water loss and extension of tomato shelf life. These findings not only expand our understanding of the involvement of β-1,3-glucanases as callose regulators in multiple developmental processes and pathogen resistance, but also provide additional insight into the manipulation of multi-agronomic traits for targeted tomato breeding.

Keywords: β-1,3-glucanase, callose, pollen/seed/fruit development, male sterility, disease resistance, tomato

Introduction

Male sterility is common in plants, mainly manifested as anther indehiscent, abnormal stamen development and gamete inactivation (Steiner-Lange et al., 2003; Ma et al.,

2018). Male sterile lines are valuable for breeding and maintaining desirable parental traits (Zhang et al., 2018). Indeed, male sterility is widely used in hybrid seed production because no artificial castration is required (Liu et al., 2001; He et al., 2019). Recently, along with deep understanding of molecular mechanism underlying how anther and pollen develop (Ge et al., 2017; Araki et al., 2020; Wu et al., 2021), breeding via male sterility has well advanced in rice (*Oryza sativa*), maize (*Zea mays*), wheat (*Triticum aestivum*) and many other food crops (Yang et al., 2019; Wan et al., 2019; Melonek et al., 2021). However, in terms of self-pollinating tomato (*Solanum lycopersicum*), it is difficult to obtain natural hybrid varieties. Therefore, any male sterile line is of great importance in tomato genetic breeding (Marti et al., 2006).

Callose is a β-l, 3-glucan polymer that are often found in plant pollen grains, pollen mother cells, endosperm cell walls, and cell plates. Dynamic callose changes play a crucial role in plant growth, development and stress response (Otegui et al., 2000; Philippe et al., 2006; Wang et al., 2010; De Storme et al., 2013; Shikanai et al., 2020; Wang et al., 2020). For instance, abnormal callose deposition can lead to pollen abortion and severe male sterility (Abad et al., 1995; Chen et al., 2017; Wang et al., 2020). In most plant species, callose is deposited between primary cell wall and plasma membrane at the corner of microspore mother cell (MMC) during the initial stages of pollen development (Suzuki et al., 2008; Suzuki et al., 2018). When MMCs undergo meiosis, callose accumulates and becomes a callose wall around MMCs. This leads to coil and isolate MMCs into a tetrahedral structure and forms tetrads that protect developing microspores (Liu et al., 2008; Zhang et al., 2014; Dou et al., 2016). In the later stage of tetrad, after degradation and disappearance of callose wall, microspores are released into the tetrad to continue their later developmental process. Thus, proper release of microspores depends on normal decomposition of callose wall (Wang et al., 2010).

Callose has also been reported to be involved in the seed endosperm development in Arabidopsis (*Arabidopsis thaliana*) and other plants (Brown et al., 1997; Otegui et al.,

2000; Philippe et al., 2006). The developmental process of endosperm includes coenocytic, cellularization, differentiation, and maturation stages (Olsen, 2001). Endosperm cellularization occurs 5-6 days after pollination in rice (Wu et al., 2016), and callose appears transiently on the cellularized endosperm cell wall, which plays an important role in endosperm cell division and differentiation (Wilson et al., 2012). However, little evidence shows callose affects seed endosperm development in tomato.

Callose biosynthesis and degradation are catalyzed by callose synthase (CALS, also known as glucan synthase like, GSL) and β-1,3-glucanase (BG), respectively (Simpson et al., 2009; De Storme and Geelen, 2014; Wu et al., 2018). In *Arabidopsis*, the *GSL* gene family consists of 12 members (Hong et al., 2001). Knockout of *AtGSL2* had little effect on vegetative growth but severely impaired callose deposition and pollen tube germination during pollen development (Dong et al., 2005). *AtGSL1* and *AtGSL5* mutants exhibit abnormal callose synthesis at the tetrad stage, resulting in callose loss and tetrad deformation (Enns et al., 2005). *AtGSL10* and *AtGSL8* can lead to callose deposition on cell plate, resulting in seedling death (De Storme et al., 2013). In contrast to GSLs, BG participates in callose decomposition and plant responses to biotic and abiotic stresses. For instance, *SbGlu1* encodes a β-1,3-glucanase that degrades callose and plays an important role in metal tolerance in sorghum (*Sorghum bicolor*) (Gao et al., 2019). In rice, inhibition of expression of β-1,3-glucanase-coding gene *Osg1* delays callose degradation during tetrad dissolution, and prevents microspore development into fertile pollens (Wan et al., 2011). Similar functions were also found for wheat BGs (Liu et al., 2015). Although more than 50 *BG* genes have been identified in *Arabidopsis*, few of them have been shown to modulate pollen or seed development. Functional analysis of BG genes in fruit crops including tomato has been even more sporadic.

Plant-originated BGs belong to the glycoside hydrolase family 17 (GH17) and are involved in regulating cell division, pollen tube germination, microspore formation, seed germination, fruit ripening and many other plant growth and developmental

processes (Roggen and Stanley, 1969; Leubner-Metzger and Meins, 2001; Nishikawa et al., 2005; Balasubramanian et al., 2012; Garcia et al., 2015; Oh et al., 2021). In addition, as important disease-processing proteins, some BGs function in plant responses to abiotic and biotic stresses (Borges et al., 2012). BGs in rice, grape (*Vitis vinifera*), wheat and other plant species have been identified based on their genetic functions and evolutionary relationships (Thomas et al., 2000; Liu et al., 2009; Rodriguez et al., 2014; Pervaiz et al., 2021). In *Arabidopsis*, the GH17 proteins are phylogenetically divided into three major clades α, β, and γ, of which the β-branch β-1,3-glucanases play important roles in microsporogenesis and pollen development (Doxey et al., 2007). Furthermore, pathogenicity-related protein 2 (PR2), a γ-branched-chain β-1,3-glucanase, affects callose deposition during *Arabidopsis* infection with *Pseudomonas syringae* (Oide et al., 2013). Another γ-branched-chain β-1,3-glucanase BG6 maintains basal callose levels as well as copper-induced reductions in keratinization and increased cytoplasmic permeability in *Arabidopsis* roots (O'Lexy et al., 2018). These studies collectively suggest that BGs possess a diverse range of functionalities in plant growth, development, and responses to biotic and abiotic stresses by affecting callose deposition. However, any specific functional importance of BGs in tomato is yet to be elucidated.

In this study, we identified a novel GH17 family gene *SlBG10*. It encodes a β-1,3-glucanase that catalyzes the hydrolysis of β-1,3-glucan and degrades callose. *SlBG10*-knockout tomato lines produced inactivated pollens and showed male sterility. We also found that *SlBG10*-knockout had substantial impact on seed production, fruit development and tomato disease resistance.

RESULTS

Characterization of *GH17* gene family identified *SlBG10* is preferentially expressed in floral buds, seeds and young fruits

GH17 proteins have been identified in *Arabidopsis* and shown to be involved in the regulation of plant growth and development (Doxey et al., 2007), while their

functions in tomato remain largely unclear. Based on amino-acid sequence identities among the conserved domain Glyco_hydro_17, we identified 50 genes that may encode GH17 family proteins in the tomato genome (SL4.0). To understand the relationships among these GH17 members, we constructed a phylogenetic tree (**Figure 1A** and **B**). As reported in *Arabidopsis* (Doxey et al., 2007), all tomato GH17s are classified into clades α, β and γ (**Figure 1A**). Clade γ contains 11 BGs that are pertinent to *Arabidopsis* homologs, some of which are involved in callose hydrolysis (Oide et al., 2013) (**Figure 1B**). We annotated these tomato clade γ homologous genes as those in *Arabidopsis*.

Expression patterns of the 11 *SlBG* genes in tomato pericarp, septum, locular, placenta, and columella tissues and developing seeds at 5, 10, 20 and 30 days post anthesis (DPA) were analyzed using RNA-seq data (Shinozaki et al., 2018). Except *SlBG10* (*Solyc11g065280*), 10 other *SlBGs* were expressed at low levels (**Figure 1C**). *SlBG10* showed relatively high expression levels in septum, locular and placenta tissues and seeds at 5, 10, and to 20 DPA. Reverse transcription quantitative PCR (RT-qPCR) was further conducted to examine relative levels of *SlBG10* transcripts in root, stem, leaf, bud, sepal, flower, seed and fruit. As shown in **Figure S1A**, *SlBG10* was preferentially expressed in seeds and buds, low in stems and leaves, and almost undetectable in roots, sepals and flowers. Interestingly, *SlBG10* was found in immature flower buds but not in open flowers, suggesting it may play a role in gamete development. Furthermore, relative amount of *SlBG10* mRNA in fruits increased dramatically at 5 DPA, peaked at 20 DPA, and then sharply decreased to an extremely low level (**Figure S1B**), which is consistent with RNA-seq results (**Figure 1C**). These findings suggest potential roles for *SlBG10* in early fruit and/or seed development. Additionally, SlBG10 was shown to localize in cytoplasm and cell membrane (**Figure 1D**).

***SlBG10*-knockout reduces fruit setting rate in tomato**

Given that *SlBG10* is highly expressed in various tomato organs and tissues (**Figure 1C; Figure S1**), we speculated that *SlBG10* may function in a wide range of tomato

growth and development processes. To examine this idea, we generated *SlBG10*-knockout mutants using CRISPR/Cas9-mediated genome editing (Liang et al., 2017; Lin et al., 2018). Among three target sites, we were able to introduce a 2-bp deletion and two 1-bp insertions into Target 3, and obtained three independent homozygous *SlBG10*-knockout lines, designated *bg10-1*, *bg10-2* and *bg10-3* (**Figure 2A**). These mutants cannot produce wild-type 338-aa SlBG10 protein, but only truncated 185-aa or 186-aa polypeptides (**Figure 2A**). We also generated *SlBG10*-transgenic lines (*SlBG10*-OE) in which *SlBG10* transcription is driven by the 35S promoter. In three representative homozygous *SlBG10*-OE lines, the transcript level of *SlBG10* was 500 to 1200 times higher than that of non-transgenic tomato, and the protein levels of SlBG10 were also higher than that of WT lines (**Figure 2B**). We next investigated whether *SlBG10* regulates tomato vegetative and reproductive growth. Wild-type (WT), *bg10*, and *SlBG10*-OE plants did not differ in plant size and anthesis time (**Figure S2A, B and C**). However, *SlBG10*-knockout mutants *bg10-1*, *bg10-2* and *bg10-3* all exhibited severely reduced fruit setting rate compared to WT and *SlBG10*-OE lines (**Figure 2C, D**). Interestingly no significant difference in fruit setting between *SlBG10*-OE and WT plants were observed. These results indicate that *SlBG10* is required and endogenous *SlBG10* level is sufficient for proper tomato fruit setting.

Pollen abortion influences fruit setting in tomato *bg10* mutants

Fruit setting can reflect degrees of plant fertility that is determined by male (stamens: anther and pollen) and female (pistils: style and ovary) reproductive organ development (Guo et al., 2016; Zhu et al., 2020; Hickerson et al., 2022). We then examined which reproductive organs are responsible for the abnormal fruit setting in *bg10* mutants. Under the same growth conditions, *bg10*, *SlBG10*-OE and WT plants exhibited no visible phenotypic changes in opened flowers including anthers, styles and ovaries (**Figure S3A**). No differences were found in anther and style lengths (**Figure S3B**), ovary morphology and ovule number (**Figure S3C**) among all plants. These results suggest that pistil is not involved in reducing fruit setting rate in *bg10*.

On the other hand, the effects of β-1,3-glucanase on pollen development have been reported in various plants (Wan et al., 2011; Liu et al., 2015). This led us to examine viability, germination and morphology of mature pollens collected from *bg10*, *SlBG10-OE* and WT tomato plants. Viability was high and showed no difference between WT and *SlBG10*-OE2 mature pollens. However, pollen viability reduced to approx. 15.49% in *bg10-1*, and almost no viable pollen was found in *bg10-2* (**Figure 3A and B**). In addition, the *ex vitro* germination rates of *bg10-1* and *bg10-2* pollens were 4.6% and 0.2%, respectively, strikingly lower than WT and *SlBG10*-OE2 pollens (**Figure 3C and D**). More than 80% WT and *SlBG10-OE2* mature pollen grains were oval and plump, with evenly distributed germination furrow. By contrast, mature *bg10* pollen grains were predominantly deformed with abnormal morphologies of shrinkage and collapse, broken pollen wall and irregular germination furrow (**Figure 3E and F**). We further performed reciprocal cross experiments between *bg10* and WT plants and tested the fertility of the *bg10* pollens and female flower buds. As shown in **Figure 3G**, *bg10* plants were able to bear fruits after pollination with WT pollen grains. However, WT plants could hardly produce any fruits after WT female flowers were pollinated with *bg10* pollen grains. These results suggest that male, but not female, fertility was compromised, and pollen abortion was responsible for the low fruit setting rate in *bg10* mutants.

SlBG10 affects pollen development by regulating callose deposition

Pollen development includes both meiotic and mitotic processes from microspore mother cell (MMC) to tetrad and from microspore separation to pollen maturation, respectively. Transition between the two processes is critical for proper pollen development (Li et al., 2015). To investigate whether *SlBG10* affects tomato pollen fertility by regulating callose content at this transition stage, we examined pollen development from MMC to uninucleate microspore in WT and *bg10* lines. As shown in **Figure 4A and B**, WT and *bg10* anthers developed normally at the MMC stage, then microspores were wrapped by callose to form a tetrad structure as described previously (Lou et al., 2014). In late tetrads, callose wall of WT anthers was gradually

degraded until microspores were released (**Figure 4C, E and I**), whilst *bg10* microspores remained tightly surrounded by callose (**Figure 4D and I**), and microspore cells began to vacuolate (**Figure 4F**). During subsequent development, WT anthers successfully formed uninucleate microspores (**Figure 4G**). However, the vacuolar microspores in *bg10* lost their nucleus and pollen grains shrunk, leading to termination of development and eventual pollen abortion (**Figure 4H**).

Furthermore, aniline blue staining assays showed that WT microspores diffused into the anther chamber at the uninucleate microspore stage and residual callus fluorescence was captured at the edge of the microspores (**Figure 4J**). In contrast, *bg10* microspores aggregated and the microspore walls showed significantly stronger callus fluorescence (**Figure 4K**). These results suggested that pollen abortion was due to the disrupted callose degradation, resulting in the failure of microspores to be released from the callus wall and premature termination of microspore development. Considering callose is mainly composed of β-1,3-glucans and is hydrolyzed by β-1,3-glucanase (Stieglitz, 1977), we then performed *in vitro* enzyme activity assays and demonstrated that SlBG10 actively hydrolyzed callose. Here SlBG10 was expressed in *E. coli* (**Figure S4**), and found to have the expected enzymatic catalytic activity to hydrolyze β-1,3-glucan (**Figure 4L**). Collectively, our results indicate that SlBG10 controls pollen development by hydrolyzing callose wall at the tetrad-to-microspore transition stage, whereas *SlBG10*-knockout causes pollen abortion and male sterility in tomato *bg10* mutants.

***SlBG10*-knockout impacts seed production in *bg10* mutants**

Pollination of *bg10* with viable WT pollens restored fruit setting, rescued male sterility, and produced fruits in crossing "*bg10* ♀× WT ♂" (**Figure 3G**). However, interestingly, in these hybrid fruits very few seeds were produced (**Figure 5A and B**). Moreover, the number (**Figure 5C**) and size (**Figure 5D**) of seeds developed in "*bg10-1* ♀ × WT ♂" and "*bg10-2* ♀ × WT ♂" fruits were significantly reduced compared to those from WT and *SlBG10*-OE2 tomatoes ($P < 0.01$, Student's *t*-tests). Many of these seeds were abortive and translucent (**Figure 5B**), and seed germination

rate was extremely low (**Figure 5E**). Mutant *bg10-1* seeds displayed similar phenotypes in these few fruits produced by naturally self-pollination (**Figure S5**). Taken together, our data reveal that *SlBG10* has a direct and indispensable function in seed development.

Callose deposition in embryo is associated with early seed development

To uncover how *SlBG10*-knockout blocks seed development, we sectioned WT and *bg10-1* fruits (ovaries) that were collected at 0, 5, 10, and 15-DPA, and defined when seed abortion occurred. As shown in **Figure 6A**, ovule and embryo morphology did not differ substantially between WT and *bg10-1* at anthesis (0-DPA) and 5-DPA. During WT embryonic development, seeds grew rapidly during 5-15 DPA, and seed structures continued to form properly, consistent with the onset of *SlBG10* expression during early seeds development (**Figure 1C**). However, development of embryos in *bg10-1* fruits stagnated at 5-10 DPA, and irregular seed structure and shape were formed.

It has been reported that endosperm cellularization occurs 5-6 days after pollination in rice (Wu et al., 2016), and callose appears transiently to the walls of the cellularized endosperm in barley (*Hordeum vulgare*) (Wilson et al., 2012). This led us to investigate whether *SlBG10* may affect callose deposition in the tomato endosperm wall at this stage as well. WT and *bg10* seeds at 5 and 10 DPA were stained with aniline blue, and WT and *bg10* endosperm cell walls showed callus fluorescence at 5-DPA (**Figure 6B**). However, no obvious callus fluorescence was seen in WT endosperm cell wall, whilst *bg10-1* maintained strong callus fluorescence at 10 DPA (**Figure 6B**), evidenced by significant differences in quantitative fluorescence intensity (**Figure 6C**). Furthermore, expression of seed development-related genes *LATE EMBRYOGENESIS ABUNDANT1* (*EM1*), *LATE EMBRYOGENESIS ABUNDANT6* (*EM6*), *SWEET15*, *MBP3*, *ABA INSENSITIVE3* (*ABI3*) and *SOMNUS* (*SOM*) were all suppressed in *bg10* mutant (**Figure 6D**). These results suggest that *SlBG10*-knockout fails to degrade calloses on endosperm cell wall. Instead, callose accumulates and results in abnormal endosperm cell differentiation that arrests early

seed development.

SlBG10-knockout enhances disease resistance in tomato fruits

Knockdown of *Arabidopsis PR2* (*At3g57260*), an *SlBG10* homolog, promotes callose deposition and enhances resistance to pathogens (Oide et al., 2013). To investigate the potential role of *SlBG10* in tomato disease resistance, we infected tomato fruits with *Botrytis cinerea*. *Botrytis* infection induced *SlBG10* expression (**Figure 7A**). Moreover, disease development was much slower on *bg10* than WT fruits, indicating *bg10* fruits were more resistance to *B. cinerea* (**Figure 7B**). Quantitative real-time PCR (qPCR) with DNA extracted from infected tomatoes confirmed significantly higher amounts of *Botrytis* in WT fruits than in *SlBG10*-knockout fruits (**Figure 7C**). We further determined the oxidative response and ability to cope with stress in *bg10* vs WT tomatoes treated with *B. cinerea*. Both *bg10-1* and *bg10-2* showed consistent upregulation of the SOD, POD and CAT enzymatic activities compared with WT (**Figure 7D**). In addition, WT and *bg10* fruit pericarps were stained with aniline blue. The cell walls of the *bg10-1* and *bg10-2* showed clear callus fluorescence compared with WT, suggesting a similar callose accumulation in anthers and seeds (**Figure 7E**). Meanwhile, expression levels of disease resistance-related genes *PR1*, *PR1a*, *PR1b*, *PR5*, *MYC2* and *NPR1* were significantly up-regulated in the mutants (**Figure 7F**), indicating that loss of *SlBG10* promoted callose accumulation to combat *B. cinerea* infection.

SlBG10-knockout increases fruit firmness and extends shelf-life

Callose is a well-known permeability barrier and leak sealant, and able to resist compression stress in plant cells (Parre and Geitmann, 2005). The increased accumulation of callose in *bg10* mutant cells (**Figure 4; Figure 6; Figure 7**) suggests that it may affect such physico-chemical properties to change tomato firmness and shelf-life, two important agronomic traits in *bg10* fruits. To test this hypothesis, we investigated the role of *SlBG10* in post-harvested fruits and their storage. We measured firmness of fruits that were collected from WT and *bg10* plants at three

ripening stages (Br, Br+3 and Br+7) using a texture analyzer. The firmness was significantly higher for *bg10* than WT fruits at all ripening stages, and decrease in *bg10* fruit firmness progressed relatively slowly (**Figure 8A**). Compared with WT, the pericarp of *bg10* fruits shrank and withered to a less extend after storage for 40 days at room temperature (**Figure 8B**). During the 40-days storage period, fruits were weighted every 5 days, and the water loss rate of *bg10* fruits was much lower (**Figure 8C**). This is consistent with increased cuticle thickness that is highly associated with water loss and fruit firmness (Li et al., 2022), in *bg10* in comparison with WT tomato pericarp tissues (**Figure 8E**). In addition, by observing fruit cells, we found that the number of cell layers (**Figure S6A and B)** and cell size (**Figure S6A and C)** were higher in *bg10* than WT tomato pericarps. These findings prompted us to examine the expression of genes related to fruit softening and cuticle synthesis. The transcript levels of *PECTATE LYASE* (*PL*), *POLYGALACTURONASE 2a* (*PG2a*), *EXPANSIN1* (*EXP1*), *CEL2*, *XYLOGLUCAN ENDOTRANS HYDROLASE 5* (*XTH5*), *XYLOGLUCAN ENDOTRANS HYDROLASE 8* (*XTH8*) and *PECTIN METHYLESTERASE 1.9* (*PME1.9*) encoding critical regulators of cell wall degradation were drastically reduced in *bg10* versus WT fruits (**Figure 8D**), while the transcript levels of the genes *GLYCEROL-3-PHOSPHATE ACYLTRANSFERASE 6* (*GPAT6*), *CYTOCHROME P450 86A* (*CYP86A*), *ECERIFERUM6* (*CER6*) and *PASTICCINO 2* (*PAS2*) encoding cuticle synthesis were significantly increased. These results further demonstrate the repressive role of *SlBG10* in regulating fruit firmness in tomato. Overall, *SlBG10*-knockout leads to marked decrease in cell wall-hydrolase gene expression and evident increase in pericarp epidermal thickness, resulting in enhancement of fruit firmness, reduction of fruit water loss and extension of fruit shelf life.

Discussion

As a polysaccharide in the form of β-1,3-glucan that can be transiently and reversibly deposited around cell wall of microspore cells, endosperm cells, and pollen grains (Wilson et al., 2006; Dou et al., 2016; Wang et al., 2020), the homeostasis of cellular

callose is maintained by balanced activities of callose synthase (CALS) vs β-1,3-glucanase (BG). Although BGs relevant to various physiological processes have been functionally characterized in *Arabidopsis* (Nishikawa et al., 2005; Doxey et al., 2007; Oide et al., 2013), little is known about involvement of BGs in plant growth, development and disease resistance in tomato. In the present study, we unravel multifunctionalities of *SlBG10,* a member of *BG* family, in pollen, seed and fruit development as well as disease resistance by regulating callose deposition in tomato.

Through comparative bioinformatic analyses, we have identified 50 *GH17* family genes in tomato. One of these genes, namely *SlBG10*, encoding β-1,3-glucanase, is highly expressed in tomato floral buds, fruits and seeds (**Figure S1**). Such tissue-specific expression profiles suggests that *SlBG10* may be involved in regulating multiple developmental processes by hydrolyzing callose in tomato. Interestingly, *bg10* exhibited male sterility and seedless fruits with improved disease resistance and firmness, and substantially extended shelf life. However, the effects of *SlBG10*-OE on these agronomic traits were not obvious, which may be due to the inconsistency between the protein accumulation and transcript levels of the OE lines. Although the transcript level of *SlBG10* was high in the OE lines, the protein level was relatively low (**Figure 2B**). Nevertheless, it also does not rule out the possibility that the level of endogenous *SlBG10* expression is sufficient and may signifies as threshold for *SlBG10* to fulfil its biological functions in tomato.

Pollen abortion usually occurs at the tetrad stage. Mature microspores are surrounded by callose walls and subsequently released from tetrads (Johns et al., 1992; Li et al., 2006; Begcy et al., 2019). BG catalyzes the hydrolysis of β-1,3-glucan to degrade callose during normal tetrad dissolution, however, BG defect can lead to male sterility (Wan et al., 2011). This is consistent with our observation that when *SlBG10* was knocked out, callose was invariably deposited around microspores, and tetrads could not be disintegrated in time, causing microspores to deform at the uninucleate microspore stage (**Figure 4)**. Furthermore, *bg10* plants were able to set and bear fruits after pollination with WT pollen grains, indicating that male but not female

reproductive organs is responsible for the reduced fecundity of *bg10* plants (**Figure 3G**). Indeed, different tissues in *bg10* and "*bg10* ♀ × WT ♂" pistils showed normal development. These results provide a molecular basis for understanding male sterility and for creating male sterile lines in tomato.

Prominent *SlBG10* expression during early seed development suggests potential involvement of *SlBG10* in seed development (**Figure 1C)**. Interestingly, seed abortion occurred not only in fruits produced by self-pollination in *bg10* (**Figure S5**) but also in "*bg10* ♀ × WT ♂" hybrid fruits (**Figure 3G**), indicating that viable WT pollen could not rescue seed development arrest. This rules out any possibility that seed abortion in *bg10* and "*bg10* ♀ × WT ♂" was caused by male sterility as previously described (Chen et al., 2018; Wu et al., 2022). Furthermore, callose hydrolysis by BGs has been reported to be involved in regulation of endosperm cell development at cellularization stage in *Arabidopsis* and other plants (Brown et al., 1997; Otegui et al., 2000; Philippe et al., 2006). However, little evidence suggests whether this would be the same case in tomato. In this regard, we have demonstrated that SlBG10 plays a key role in endosperm development by regulating the hydrolysis of callose at cellularization stage. *SlBG10*-knockout caused abnormal callose deposition in endosperm cell wall, leading to arrest early embryo development to generate seeds. Surprisingly, *SlBG10* performs similar functions during pollen and seed development via degradation of callose wall surrounding microspores or endosperm cells. It is known that calloses increase the plasticity of the endosperm and microspore cell walls to provide spatial isolation and protect fragile dividing and differentiating cells (Otegui et al., 2000; Weier et al., 2014). As these cells reach their mature stage, BGs hydrolyze callose coils, leading to successful completion of the entire developmental process (Stieglitz, 1977). Nevertheless, in contrast to other well-studied cell wall substances such as pectin and cellulose (Ye et al., 2020; Wang et al., 2022), detailed mechanism by which callose regulates tomato seed growth and development requires further investigation.

SlBG10-knockout imposes marked effects on fruit development, postharvest fruit

quality, and disease resistance in tomato (**Figure 7 and 8**). This is evident by changes in several agronomic traits including increase in fruit firmness and cuticle thickness, reduction and delay in water loss during tomato storage, and enhance resistance to *B. cinerea* in *bg10* mutants. Consistent with increased firmness, genes related to cell wall softening, such as *PL*, *PG2a*, and *EXP1*, were significantly downregulated in the *bg10* mutants ($P < 0.05$, Student's *t*-tests). Cuticle thickness is also known to be positively associated with firmness (Li et al., 2022). Indeed, numbers of cell layers and cell sizes of pericarp increased substantially, which may have contributed to the increased *bg10* fruit firmness. However, how callose affects fruit firmness is unclear. Nevertheless, thick pericarp, high firmness and few-locular gel content are common in seedless tomatoes (de Jong et al., 2009; Olimpieri et al., 2011; Zhang et al., 2019; Huang et al., 2021; Wang et al., 2022). Contrary to the common perception that fruit development is independent of seed formation, our findings described in this report along with others (de Jong et al., 2009; Olimpieri et al., 2011; Zhang et al., 2019; Huang et al., 2021; Wang et al., 2022) suggest that how seed develops in tomato may have some retro-influences on fruit development. On the other hand, downregulation of the *SlBG10* homolog *PR2* in *A. thaliana* leads to the accumulation of callose and enhances leaf resistance to pathogens (Oide et al., 2013). We have now extended the disease resistance spectrum to fruits where *SlBG10*-knockout increases defense against *B. cinerea* infection in *bg10* mutants.

Male sterility and seedlessness are important traits in fruit crop breeding (Martinelli et al., 2009; Chang et al., 2016). *SlBG10* mutations can lead to male sterility, seedless fruits, and improved postharvest fruit traits. This opens opportunities to use *bg10* as female parents in tomato breeding. Furthermore, different mutant *bg10* lines exhibit different phenotypic intensities. Indeed, unlike *bg10-2* and *bg10-3*, *bg10-1* does not cause complete seed abortion and it can still produce a limited number of viable seeds. This line has particular potentials as breeding material to produce hybrid offspring. In summary, this study not only expands our understanding of the involvement of β-1,3-glucanases as callose regulators in multiple developmental

processes and disease resistance, but also describes a gene controlling key agronomic traits for tomato breeding.

Materials and Methods

Identification of GH17 family members

The Pfam domain of the conserved GH17 domain (PF00332) was used to identify the tomato (*Solanum lycopersicum*) GH17 family (Mistry et al., 2021), and the GH17 protein sequences of *Arabidopsis thaliana* and *Solanum lycopersicum* were retrieved by HMMER software (Marchin et al., 2005). Protein sequence alignments were performed using MEGA X, and phylogenetic trees of the GH17 family proteins were constructed by the Maximum Likelihood (ML) method (Kimura 1980). The bootstrap consensus tree was inferred from 1000 replicates (Felsenstein 1985). Branches corresponding to partitions reproduced in < 50% bootstrap replicates were collapsed.

Plant growth conditions and genetic transformation

Wildtype and transgenic tomato plants (*S. lycopersicum* L. cv MicroTom) used in this study were grown in an insect-free greenhouse with the conditions described in Deng et al. (2022). Coding sequence of the SlBG10-tagged with 3xFlag fusion protein was cloned into the pBI121 vector to generate *SlBG10*-OE constructs using a homologous recombination clone kit (Vazyme, China). CRISPR/Cas9-mediated genome editing was performed as previously described (Deng et al., 2022). Three target sequences of *SlBG10* were designed with the CRISPR-P online tool (http://crispr.hzau.edu.cn/cgi-bin/CRISPR2/CRISPR). Double-stranded DNA of target sequences was generated by PCR and cloned into pFASTCas9/ccdB binary vector using a Golden Gate Assembly kit. The final constructs pBI121-SlBG10-OE, and pFASTCas9/ccdB-SlBG10 were confirmed by Sanger sequencing and transformed into the tomato cultivar MicroTom via *Agrobacterium tumefaciens*-mediated transformation (Deng et al., 2022).

In T1 generation, Kanamycin-resistant seedlings were transferred to composts and grown in insect-free greenhouse. Transgenes were verified by genomic PCR to detect T-DNA insertion and RT-PCR assays of transgene expression. Gene editing in

seedlings was confirmed by PCR, cloning and sequencing of the three targeted genomic regions. PCR products were sequenced directly, and the superimposed sequencing chromatograms were decoded manually or using the automated web tool DSDecodeM (http://skl.scau.edu.cn/dsdecode/).

Gene expression analyses

RNA-seq data used for expression analysis were obtained from the SGN database (https://solgenomics.net/) (Shinozaki et al., 2018). Quality reads were controlled and trimmed using fastp (Chen et al., 2018). Paired reads were mapped to the tomato reference genome SL4.0 with the ITAG4.0 annotation using HISAT 2 with default parameters (Kim et al., 2015). Counts of reads per gene was calculated using the FeatureCount program. These results were aggregated to obtain gene-level expression estimates in units of transcripts per million (TPM). Heat maps for expression levels of *SlBG10* and other γ-branch genes in different tissues at various developmental stages were constructed (Chen et al., 2020).

Subcellular localization

Subcellular localization of SlBG10 was investigated as described previously (Deng et al., 2018). Full coding sequence of *SlBG10* without stop codon was amplified and inserted into a vector harboring 35S:GFP. The 35S:SlBG10-GFP construct and the empty 35S:GFP vector were infiltrated into leaves of *Nicotiana benthamiana* using a 1 mL needle-free syringe. After incubation at 22 °C for 48 h in the dark, GFP fluorescence signal was observed under a fluorescence microscope (DM4 B, Leica, Germany) (brightfield: 10 ms exposure; green fluorescence at a laser intensity of 30 %: 500 ms exposure).

Phenotypic analysis of tomato tissues

Five plants were randomly selected from each treatment, and then ten flowers from each plant were randomly selected for counting fruit-set rates. Sizes of plants (50 days after germination) were measured using a cursor caliper. Anthers, styles, and seeds (at Br+7 stage) were observed and photographed under a stereomicroscope (M205FA,

Leica, Germany), and diameters of different tissues were measured using ImageJ software.

Pollen viability and germination assays

Pollen viability was measured using Alexander stain (Coolaber, Beijing) (Peterson et al., 2010) and 1% iodine-potassium iodide solution ($KI-I_2$). Pollens were placed on slide, mixed with 2-3 drops of dye solution, and immediately covered with thin cover glass. Pollen grains were then observed and photographed under a stereoscopic microscope (M205FA, Leica, Germany). Pollen germination experiments were carried out on pollen germination agar-medium as described previously (Boavida and McCormick et al., 2007; Vogler et al., 2014). Five microscopic fields were randomly selected, numbers of viable, non-viable, and germinating pollen grains of each treatment were counted under a stereoscopic microscope (M205FA, Leica, Germany).

Electron microscopy

For scanning electron microscopy (SEM), mature pollens were collected from WT, *bg10* and *SlBG10*-OE lines, mounted on a copper specimen holder using the conductive glue. Pollens were subsequently subjected to the critical point drying with CO_2 (EM CPD300, Leica, Germany) before being gold-coated, and observed under an Apreo S electron microscope (Thermo scientific, Netherlands) and photographed at different magnifications.

Histological analysis

Anthers at four developmental stages as described previously (Chen et al., 2018) (I, bud < 2mm in diameter, microspore mother cell stage; II, bud 2.5–3.5mm, tetrad stage; III, bud 3.6–4.5mm, early uninucleate microspore stage; IV, bud 4.6–5.5mm, uninucleate microspore stage) were collected and fixed in FAA solution containing 3.7% paraformaldehyde (v/v), 50% ethanol (v/v) and 5% acetic acid (v/v) in 1× PBS, then dehydrated in alcohol before being embedded in paraffin and sectioned. Sections were immersed into safranin O staining solution and fast green staining solution for 4-6s, respectively. Tissue sections were mounted with neutral balsam and observed

under a fluorescence whole slide imaging system (Olympus VS200, Japan). This method was also used to histologically examine ovary, pericarp and seeds of WT, *bg10* and *SlBG10*-OE lines. In addition, Pericarp were hand-sectioned, mounted on glass slides, stained with 0.5% Toluidine blue (w/v) for 30s, and observed under a stereomicroscope (M205FA, Leica, Germany). Numbers and sizes of cells were quantified using ImageJ software. To observe fruit cuticles, fruits were collected from each line at mature green stage, cryo-sectioned, dried at room temperature for about 15min, then stained with oil-saturated O liquid for 8-10 minutes. Sections were sealed with glycerin gelatin and observed under Olympus VS200. Cuticle thickness was measured and calculated using ImageJ.

Reciprocal crossing experiments

Reciprocal crosses between *bg10* and WT plants were performed under glasshouse conditions using manual emasculation of immature female flower buds followed by paper-bag isolation. Tomato pollens from WT plants were collected and used to fertilize emasculated *bg10* line. Pollens from *bg10* line were used to fertilize the stigma of emasculated WT flowers, WT×WT plants were used as control. Fruit-setting events in pollinated plants were counted ten days after crossing.

Callose staining with aniline blue

To determine the callose content in different tissues between WT and *bg10* lines, aniline blue staining of callose was performed as described by Conrath et al. (1998). Sectioned anthers, seeds and pericarps were stained with aniline blue solution and observed under a fluorescence whole slide imaging system (Olympus VS200, Japan). Callose deposition was quantified by fluorescence of callose deposits using ImageJ software, and 'Histogram list' as the reference for calculating fluorescence intensity (Ellinger et al., 2013).

Enzyme activity assay

Coding sequence of *SlBG10* was cloned into pET28a vector. Recombinant plasmid was transformed into *E. coli* BL21 (DE3). Positive transformants were collected and

incubated at 37°C until OD_{600} reached 0.6-0.8. Isopropyl β-D-1-thiogalactopyranoside (IPTG) was added to bacterial cultures to induce SlBG10 expression at 16°C, and 1 ml of bacteria cultures was collected every hour for Sodium dodecyl sulfate–polyacrylamide gel electrophoresis (SDS-PAGE). After 6 hours, bacteria were collected by centrifugation at 5,000 g for 10 min at 4°C, re-suspended in PBS buffer, and treated by ultrasonic crusher. After centrifugation, supernatant was collected and filtered through an 0.45-μm membrane filter. Protein concentration was determined using the Bradford Protein Assay Kit (Beyotime, Shanghai). Hydrolytic activity of SlBG10 was determined by the dinitrosalicylic acid (DNS) method (Miller, 1959). The reaction mixture (200 μL), containing 0.1% (w/w) laminarin (a β-1,3-glucan; Coolaber, Beijing, China) dissolved in phosphate buffer (50 mM, pH 6) and 20 μL enzyme liquid (2.5mg/mL induced protein solution) or reference solution (2.5mg/mL uninduced protein solution) was incubated for 3 h at 42°C. Then, 200 μL DNS was added to terminate the reaction. The resulting mixture was boiled for 5 min at 100°C. Absorbance of reducing sugar at wavelength of 520nm was determined by a Thermo Multiskan go (Thermo scientific, USA) after the reaction product was cooled to room temperature. One enzyme activity unit (1U) was defined as the amount of enzyme required to produce 1 μmol of glucose per minute under the above reaction conditions.

RNA isolation and RT-qPCR analysis

The plant RNA extraction kit (BIOFIT, Chengdu) was used to isolate total RNA from different tomato tissues. Seed and pericarp RNA were extracted to analyze the expression of genes related to seed development, fruit firmness and disease-resistance, respectively. RNAs from roots, stems, leaves, flowers, buds and fruits in different stages were also extracted to analyze the tissue-specific expression of *SlBG10*. Reverse transcription and genomic DNA-removal were performed as described (Deng et al., 2022). RT-qPCR was performed using 2×SP qPCR Mix (Bioground, Chongqing) on a Bio-rad CFX96 Real-Time PCR System (BIO-RAD, USA), and the primers used in the expression analyses are listed in Supplementary Table S1. Each

type of detections was performed on three biological and three technical replicates.

Western blot analysis

Total protein extraction and western blot analysis were performed as previously described (Pasoreck et al., 2016; Fernandez-San et al., 2019). Fruit tissues were collected and ground to powder in liquid nitrogen and extracted using protein extraction buffer containing 0.5 M Tris–HCl (pH 6.5), 4% SDS (w/v), 20% glycerol (v/v) and 10% β-mercaptoethanol (v/v). Proteins were separated on 10% polyacrylamide gels by SDS-polyacrylamide gel electrophoresis (PAGE). Anti-DYKDDDDK antibody was used for Western blot detection at a dilution ratio of 1:5000. Chemiluminescence detection was performed using an ECL Western Blotting Detection kit (Bioground, Chongqing).

Postharvest water loss analysis

To evaluate the fruit shelf-life of *SlBG10*-OE and *bg10* lines, 20 fruits were harvested at 7 days after breaker (Br+7d). Fruits were then kept in an incubator supplemented with light (22°C, 16-h light period), and every single fruit was weighed immediately after harvest and then weighed every 10 days until 60 days. Water loss rate was calculated as the ratio of the decreased fruit weight to the initial fruit weight (Ji et al., 2014).

Fruit firmness

At least 20 fruits at breaker (Br), breaker+3d (Br+3) and breaker+7d (Br+7) stages were randomly assigned for each line. Fruit firmness was determined using a texture analyzer (TA.XTC-18, BOSIN, Shanghai).

Statistical analysis

All data are expressed as mean ± standard deviation (SD) from three or more independent experiments and subjected to the student's *t*-test for pairwise comparison or ANOVA for multivariate analysis.

Pathogen inoculation

Representative *Botrytis cinerea* strains were isolated from tomato leaves. Inoculation of *B. cinerea* was performed as described previously (Pei et al., 2019). Fruits of wild type, *bg10-1* and *SlBG10*-OE were surface-disinfected with 75% ethanol (v/v) and washed twice with sterilized distilled water, respectively. Mycelial plugs of *B. cinerea* were adhered on each wounded leaves and fruits (slightly stabbed by anatomic needle). Inoculated tomato fruits were kept in a moistened growth chamber at 20°C with a 12 h light/12 h dark cycle. At one day after inoculation, mycelial plugs were removed from inoculated tomato tissues. At least 20 leaves and fruits were tested for each treatment and an equal number of controls inoculated only with agar plugs were included. Total DNA was extracted from WT and *bg10* fruits after inoculation with *B. cinerea*. And DNA (50ng) was used for qPCR and the ratio of *B. cinerea AgDNA* to tomato *ACTIN* gDNA was measured as previously described (Zhang et al., 2013).

Antioxidant enzyme activity

The activity levels of antioxidant enzymes such as SOD, POD and CAT are indicative of plant disease resistance (Yang et al., 2017; Sun et al., 2018). The enzymatic activities of SOD, POD and CAT were quantified using relevant assay kits (Solarbio, Beijing) following the manufacturer's instructions, and the optical density was measured at 560-, 470- and 240-nm using a Thermo Multiskan go (Thermo scientific, USA), respectively.

Accession Numbers

Sequence data from this article can be found in the Tomato Genome Protein Sequences (ITAG release 4.0) database under the following accession numbers: *SlBG10* (*Solyc11g065280*), *SlBG1* (*Solyc01g060020*), *SlBG2* (*Solyc01g060010*), *SlBG3* (*Solyc10g079860*), *SlBG4* (*Solyc03g025650*), *SlBG5* (*Solyc03g025645*), *SlBG6* (*Solyc01g059965*), *SlBG7* (*Solyc01g008620*), *SlBG8* (*Solyc01g008610*), *SlBG9* (*Solyc02g086700*), *SlBG11* (*Solyc11g065290*), *Actin* (*Solyc11g005330*), *EM1* (*Solyc09g014750*), *EM6* (*Solyc06g048840*), *SWEET15* (*Solyc09g074530*), *MBP3* (*Solyc06g064840*), *ABI3* (*Solyc06g083600*), *SOM* (*Solyc07g053750*), *PR1* (*Solyc09g007010*), *PR1a* (*Solyc01g106620*), *PR1b* (*Solyc01g106610*), *PR5*

(*Solyc08g080670*), *NPR1* (*Solyc07g040690*), *MYC2* (*Solyc08g076930*), *PL* (*Solyc03g111690*), *PG2a* (*Solyc10g080210*), *EXP1* (*Solyc06g051800*), *CEL2* (*Solyc09g010210*), *XTH5* (*Solyc01g081060*), *XTH8* (*Solyc04g008210*), *PME1.9* (*Solyc07g064170*), *GPAT6* (*Solyc09g014350*), *CYP86A* (*Solyc06g076800*), *CER6* (*Solyc02g085870*) and *PAS2* (*Solyc04g014370*).

Supplemental Data

Supplemental Figure S1. Expression pattern of *SlBG10* during tomato development.

Supplemental Figure S2. Vegetative growth and anthesis of WT, *bg10* and *SlBG10*-OE lines.

Supplemental Figure S3. Characterization of opened flower in WT, *bg10* and *SlBG10*-OE lines.

Supplemental Figure S4. *E. coli* cultures at different incubation times were analyzed by SDS-PAGE to determine the induced expression of SlBG10.

Supplemental Figure S5. Fruits of *bg10-1* and WT at different developmental stages.

Supplemental Figure S6. Transverse sections of WT and *bg10* fruits at 30-DPA.

Supplemental Table S1. The primers used in the experiments.

Funding Information

This research was supported by the National Natural Science Foundation of China (32172643 and 32172271), Applied Basic Research Category of Science and Technology Program of Sichuan Province (2021YFQ0071, 2022YFSY0059, and 2021YFYZ0010-5), Technology Innovation and Application Development Program of Chongqing (cstc2021jscx-cylhX0001), and this project is also supported by the Fundamental Research Funds for the Central Universities (SCU2022D003).

Conflict of interests. The authors declare no conflict of interest.

Author contributions

M.L., Y.P. and Q.X. planned and designed the research; Y.P., Q.X., and Z.Z. performed experiments; P.S. and H.D. analyzed data; Y.P., M.L. and Y.H. wrote the manuscript and M.B. helped improve the manuscript.

Figure legends

Figure 1. Identification of tomato GH17 genes. A, Phylogenetic tree of GH17 family proteins from tomato. All family members are divided into three clades, represented by different colors. B, Phylogenetic tree of β-1,3-glucanases of clade γ from *Arabidopsis thaliana* and *Solanum lycopersicum*. Proteins from different sub-clades are labeled with colored dots. C, Heatmap representation of the relative expression of clade γ genes in different tissues and developmental stages of tomato. DPA stands for days post-anthesis. D, Subcellular localization of SlBG10. *SlBG10* in-frame fused to green fluorescence protein (GFP) and free GFP were transiently expressed in *Nicotiana benthamiana* leaf epidermal cells.

Figure 2. *SlBG10* is required for fruit setting in tomato. A, Outlines of *SlBG10*-knockout mutations generated by the CRISPR/Cas9 genome editing system. Three sequences targeting *SlBG10* were designed and three mutant-types of homozygous T1 lines *bg10-1*, *bg10-2* and *bg10-3* with premature translation stop codons were obtained. Orange boxes indicate the location of Targets 1-3. The sequences of Target 3 are highlighted blue. Domain of SlBG10, nucleotide deletion or insertion, as well as amino-acid (aa) sequences of WT and truncated SlBG10 are indicated. B, Relative *SlBG10* transcript levels in WT and *SlBG10* overexpression (*SlBG10*-OE) lines and Western blot analysis of SlBG10 protein levels in WT and *SlBG10*-OE lines. C and D, Fruit setting rate in WT, *bg10*, and *SlBG10*-OE lines. Photographs were taken at 25-DPA. Data are presented as means ± SD (n = 3 in B, n = 6 in D). Student's ***t***-tests were performed and p values of *P < 0.05, **P < 0.01 indicate statistically significant when compared to WT.

Figure 3. *SlBG10*-knockout *bg10* mutants exhibit reduction of pollen viability, germination rate and abnormal morphology compared to WT and *SlBG10*-OE lines. A, KI-I_2 (upper panel) and Alexander (lower panel) staining of mature pollens collected from WT, *bg10-1*, bg10-2 and *SlBG10*-OE2 lines. Pollen grains that were viable stained black, while dead pollen grains stained yellow or light red by KI-I_2. Pollen grains that were viable stained dark blue or purple, while dead pollen grains were stained pale turquoise blue by Alexander. B, Percentage of viable pollen. C, *Ex-vitro* germination of mature pollens on pollen germination medium. D, Germination rate of mature pollens. E, SEM micrographs of pollen grains collected from WT, *bg10-1*, *bg10-2* and *SlBG10*-OE2 lines, respectively. F, Percentage of normal pollens. G, Reciprocal cross experiments between *bg10* and WT plants. Signs ♂ and ♀ represent male and female parent, respectively. Oval-shaped and shriveled pollens produced by WT plants or *bg10* lines are either viable or dead, respectively. Data are shown as means ± standard deviation (SD) (n = 5). Student's ***t***-tests were performed and p values of *P < 0.05, **P < 0.01 indicate statistically significant when compared to WT.

Figure 4. *SlBG10*-knockout *bg10* mutants display aberrant development of pollen and SlBG10 affects callose deposition around pollen grains. A-H, Histological observation of pollen development during microspore mother cell (MMC) to uninucleate microspore transition stage in WT and *bg10* lines. MMC, microspore mother cell; T, tapetum; Td, tetrad; Msp, microspore; dMsp, degenerated microspore; c, callose. I, Tetrads begin to degrade and microspores were released from callose wall in WT line, whilst callose deposition continued in the *bg10* mutant. J, Callose deposition was visible in aniline blue-stained anthers from WT and bg10 lines under the fluorescence microscopy. The stronger fluorescence indicates the more callose deposits. K, Relative fluorescence Intensity of pollens from WT and *bg10* lines. L, Enzyme activity of SlBG10 to hydrolyze callose (β-1,3-glucan). Laminarin was used as substrate. Total proteins extracted from *E. coli* without or with IPTG induction were used as the negative control (CK) or SlBG10 enzymatic solution, respectively.

Data are shown as means ± SD (n = 6 in D; n = 3 in E). Student's ***t***-tests were performed and p values of *P < 0.05, **P < 0.01 indicate statistically significant when compared to CK.

Figure 5. *SlBG10*-knockout *bg10* mutants exhibit seed abortion phenotype. A, Fruit sections of WT, *bg10-1*, *bg10-2* and *SlBG10*-OE2 lines. Fruits from *bg10-1*, *bg10-2* lines are seedless but mature seeds are produced in WT and *SlBG10*-OE line. B, Morphology of mature seeds from different lines. C, Number of seeds per fruit. D, Size of seeds. In the boxplots, the center line, box limits and whiskers denote the median, upper and lower quartiles and 1.5 × interquartile range, respectively. E, Seed germination rate. Data are shown as means ± SD (n = 20 in D and E; n = 3 in F), Student's ***t***-tests were performed and p values of *P < 0.05, **P < 0.01 indicate statistically significant when compared to WT.

Figure 6. Abnormal callose deposition in the embryo results in early seed abortion. A, Transverse sections of fruits and seeds of WT and *bg10-1* line at anthesis (0-DPA), 5, 10 and 15 DPA. B, Callose deposition was visible in aniline blue-stained seeds from WT and bg10 lines under the fluorescence microscopy (BF, bight filed; DAPI, DAPI fluorescence; Merge, merge of DAPI and BF). C, Relative fluorescence intensity of seeds of WT and bg10 lines. D, Relative expression levels of seed development-related genes *EM1*, *EM6*, *SWEET*, *MBP3*, *ABI3* and *SOM* in WT and *bg10* lines. Data are shown as means ± standard deviation (SD) (n = 6 in C; n = 3 in D), Student's ***t***-tests were performed and p values of *P < 0.05, **P < 0.01 indicate statistically significant when compared to WT.

Figure 7. Disease resistance of *bg10* fruits. A, Induction of *SlBG10* expression by *Botrytis cinerea*. CK, blank PDA media. B, Disease symptoms on WT and *bg10* fruits at 48-hours after inoculation with mycelial plugs of *B. cinerea*. And the lesion diameter of tomato fruits. C, The ratio of *Botrytis* DNA to tomato DNA on WT and *bg10* fruits at 48-hours after inoculation with *B. cinerea*. D, Antioxidant enzymatic activities of SOD, POD and CAT after inoculation with *B. cinerea*. E, Callose deposition was visible in aniline blue-stained fruit pericarps from WT and *bg10* lines

under the fluorescence microscopy. F, Relative expression levels of disease-resistance related genes *PR1*, *PR1a*, *PR1b*, *PR5*, *MYC2* and *NPR1* in WT and *bg10* lines. Data are presented as means ± SD (n = 3 in A, C, D and F; n = 6 in B). Student's t-tests were performed and p values of *P < 0.05, **P < 0.01 indicate statistically significant when compared to WT.

Figure 8. Knockout of *SlBG10* increases fruit firmness and extends shelf-life. A, Firmness of WT and *bg10* fruits at the Br (fruit at breaker), Br + 3 (3 days post-breaker) and Br + 7 (7 days post-breaker) stages. B, WT and *bg10-1* fruits harvested at BR + 7 stage and stored at 22℃. Photographs were taken at 40 days of storage. C, Lost fruit weight/fresh fruit weight ratio. In the boxplots, the center line, box limits and whiskers denote the median, upper and lower quartiles and 1.5 × interquartile range, respectively. D, Relative expression levels of fruit firmness-related genes *PL*, *EXP1*, *PG2a*, *CEL2*, *XTH5*, *XTH8* and *PME1.9* in WT and *bg10* lines. E, Cuticle thickness of WT and *bg10* fruits. F, Relative expression levels of cuticle synthesis-related genes *GPAT6*, *CYP86A*, *CER6* and *PAS2* in WT and *bg10* lines. Data are shown as means ± SD (n = 6 in A; n = 6 in C; n = 3 in E), Student's t-tests were performed and p values of *P < 0.05, **P < 0.01 indicate statistically significant when compared to WT.

References

Abad AR, Mehrtens BJ, Mackenzie SA (1995) Specific expression in reproductive tissues and fate of a mitochondrial sterility-associated protein in cytoplasmic male-sterile bean. The Plant Cell **7:** 271-285

Araki S, Le NT, Koizumi K, Villar-Briones A, Nonomura KI, Endo M, Inoue H, Saze H, Komiya R (2020) miR2118-dependent U-rich phasiRNA production in rice anther wall development. Nature communication **11:** 3115

Balasubramanian V, Vashisht D, Cletus J, Sakthivel N (2012) Plant β-1,3-glucanases: their biological functions and transgenic expression against phytopathogenic fungi. Biotechnology letters **34:** 1983-1990

Begcy K, Nosenko T, Zhou LZ, Fragner L, Weckwerth W, Dresselhaus T (2019) Male sterility in maize after transient heat stress during the tetrad stage of pollen development. Plant Physiology **181:** 683-700

Boavida LC, McCormick S (2007) Temperature as a determinant factor for increased and reproducible in vitro pollen germination in *Arabidopsis thaliana*. The Plant Journal **52:** 570-582

Borges A, Tsai SM, Caldas DG (2012) Validation of reference genes for RT-qPCR normalization in common bean during biotic and abiotic stresses. Plant Cell Reports **31:** 827-838

Brown RC, Lemmon BE, Stone BA, Olsen OA (1997) Cell wall (1→ 3)- and (1→ 3, 1→ 4)-β-glucans during early grain development in rice (*Oryza sativa* L.). Planta **202:** 414-426

Chang Z, Chen Z, Wang N, Xie G, Lu J, Yan W, Zhou J, Tang X, Deng XW (2016) Construction of a male sterility system for hybrid rice breeding and seed production using a nuclear male sterility gene. Proceedings of the National Academy of Sciences **113:** 14145-14150

Chen C, Chen H, Zhang Y, Thomas HR, Frank MH, He Y, Xia R (2020) TBtools: an integrative toolkit developed for interactive analyses of big biological data. Molecular Plant **13:** 1194-1202

Chen L, Yang D, Zhang Y, Wu L, Zhang Y, Ye L, Pan C, He Y, Huang L, Ruan YL, Lu G (2018) Evidence for a specific and critical role of mitogen-activated protein kinase 20 in uni-to-binucleate transition of microgametogenesis in tomato. New Phytologist **219:** 176-194

Chen S, Zhou Y, Chen Y, Gu J (2018) fastp: an ultra-fast all-in-one FASTQ preprocessor. Bioinformatics **34:** i884-i890

Chen R, Zhao X, Shao Z, Wei Z, Wang Y, Zhu L, Zhao J, Sun M, He R, He G (2007) Rice UDP-glucose pyrophosphorylase1 is essential for pollen callose

791 deposition and its cosuppression results in a new type of thermosensitive genic
792 male sterility. The Plant Cell **19:** 847-61

793 **Conrath U, Klessig DF, Bachmair A** (1998) Tobacco plants perturbed in the
794 ubiquitin-dependent protein degradation system accumulate callose, salicylic
795 acid, and pathogenesis-related protein 1. Plant Cell Reports **17:** 876-880

796 **Cui Y, Li R, Li G, Zhang F, Zhu T, Zhang Q, Ali J, Li Z, Xu S** (2020) Hybrid
797 breeding of rice via genomic selection. Plant Biotechnology Journal **18:** 57-67

798 **Deng H, Pirrello J, Chen Y, Li N, Zhu S, Chirinos X, Bouzayen M, Liu Y, Liu M**
799 (2018) A novel tomato F-box protein, SlEBF3, is involved in tuning ethylene
800 signaling during plant development and climacteric fruit ripening. The Plant
801 Journal **95:** 648-658

802 **Deng H, Chen Y, Liu Z, Liu Z, Shu P, Wang R, Hao Y, Su D, Pirrello J, Liu Y,**
803 **Li Z, Grierson D, Giovannoni JJ, Bouzayen M, Liu M** (2022) *SlERF*. *F12*
804 modulates the transition to ripening in tomato fruit by recruiting the co-repressor
805 TOPLESS and histone deacetylases to repress key ripening genes. The Plant Cell
806 **34:** 1250-1272

807 **De Jong M, Wolters-Arts M, Feron R, Mariani C, Vriezen WH** (2009) The
808 *Solanum lycopersicum* auxin response factor 7 (*SlARF7*) regulates auxin
809 signaling during tomato fruit set and development. The Plant Journal **57:** 160-
810 170

811 **De Storme N, Geelen D** (2014) Callose homeostasis at plasmodesmata: molecular
812 regulators and developmental relevance. Frontiers in plant science **5:** 138

813 **De Storme N, De Schrijver J, Van Criekinge W, Wewer V, Dormann P, Geelen D**
814 (2013) GLUCAN SYNTHASE-LIKE8 and STEROL
815 METHYLTRANSFERASE2 are required for ploidy consistency of the sexual
816 reproduction system in *Arabidopsis*. The Plant Cell **25:** 387-403

817 **Dong X, Hong Z, Sivaramakrishnan M, Mahfouz M, Verma DPS** (2005) Callose

synthase (CalS5) is required for exine formation during microgametogenesis and for pollen viability in *Arabidopsis*. The Plant Journal **42:** 315-328

Dou XY, Yang KZ, Ma ZX, Chen LQ, Zhang XQ, Bai JR, Ye D (2016). AtTMEM18 plays important roles in pollen tube and vegetative growth in *Arabidopsis*. Journal of Integrative Plant Biology **58:** 679-92.

Doxey AC, Yaish MW, Moffatt BA, Griffith M, McConkey BJ (2007) Functional divergence in the *Arabidopsis* beta-1,3-glucanase gene family inferred by phylogenetic reconstruction of expression states. Molecular Biology and Evolution **24:** 1045-1055

Ellinger D, Naumann M, Falter C, Zwikowics C, Jamrow T, Manisseri C, Somerville SC, Voigt CA (2013) Elevated early callose deposition results in complete penetration resistance to powdery mildew in *Arabidopsis*. Plant Physiology **161:** 1433-1444

Enns LC, Kanaoka MM, Torii KU, Comai L, Okada K, Cleland RE (2005) Two callose synthases, GSL1 and GSL5, play an essential and redundant role in plant and pollen development and in fertility. Plant Molecular Biology **58:** 333-349

Fan Y, Lin S, Li T, Shi F, Shan G, Zeng F (2022) The plasmodesmata-located beta-1,3-glucanase enzyme PdBG4 regulates trichomes growth in *Arabidopsis thaliana*. Cells **11:** 2856

Felsenstein J (1985) Confidence limits on phylogenies: an approach using the bootstrap. Evolution **39:** 783-791

Fernandez-San MA, Aranjuelo I, Douthe C, Nadal M, Ancin M, Larraya L, Farran I, Flexas J, Veramendi J (2018) Physiological performance of transplastomic tobacco plants overexpressing aquaporin AQP1 in chloroplast membranes. J Exp Bot **69:** 3661-3673

Gao J, Yan S, Yu H, Zhan M, Guan K, Wang Y, Yang Z (2019) Sweet sorghum (*Sorghum bicolor* L.) *SbSTOP1* activates the transcription of a beta-1,3-

glucanase gene to reduce callose deposition under Al toxicity: A novel pathway for Al tolerance in plants. Bioscience Biotechnology and Biochemistry **83:** 446-455

Garcia R, Botet J, Rodriguez-Pena JM, Bermejo C, Ribas JC, Revuelta JL, Nombela C, Arroyo J (2015) Genomic profiling of fungal cell wall-interfering compounds: identification of a common gene signature. BMC Genomics **16:** 683

Ge Z, Bergonci T, Zhao Y, Zou Y, Du S, Liu MC, Luo X, Ruan H, Garcia-Valencia LE, Zhong S, Hou S, Huang Q, Lai L, Moura DS, Gu H, Dong J, Wu HM, Dresselhaus T, Xiao J, Cheung AY, Qu LJ (2017) *Arabidopsis* pollen tube integrity and sperm release are regulated by RALF-mediated signaling. Science **358:** 1596-1600.

Guo Z, Slafer GA, Schnurbusch T (2016) Genotypic variation in spike fertility traits and ovary size as determinants of floret and grain survival rate in wheat. Journal of experimental botany **67:** 4221-4230

He Y, Yan L, Ge C, Yao XF, Han X, Wang R, Xiong L, Jiang L, Liu CM, Zhao Y (2019) *PINOID* is required for formation of the stigma and style in Rice. Plant Physiology **180:** 926-936

Hickerson N, Samuel MA (2022) Stylar steroids: brassinosteroids regulate pistil development and self-incompatibility in primula. Current Biology **32:** R135-R137

Hong Z, Delauney AJ, Verma DP (2001) A cell plate-specific callose synthase and its interaction with phragmoplastin. The Plant Cell **13:** 755-768

Huang B, Hu G, Wang K, Frasse P, Maza E, Djari A, Deng W, Pirrello J, Burlat V, Pons C, Granell A, Li Z, van der Rest B, Bouzayen M (2021) Interaction of two MADS-box genes leads to growth phenotype divergence of all-flesh type of tomatoes. Nature communication **12:** 6892

Ji K, Kai W, Zhao B, Sun Y, Yuan B, Dai S, Li Q, Chen P, Wang Y, Pei Y, Wang

H, Guo Y, Leng P (2014) *SlNCED1* and *SlCYP707A2*: key genes involved in ABA metabolism during tomato fruit ripening. Journal of experimental botany **65:** 5243-5255

Johns C, Lu M, Lyznik A, Mackenzie S (1992) A mitochondrial DNA sequence is associated with abnormal pollen development in cytoplasmic male sterile bean plants. The Plant Cell **4:** 435-449

Kim D, Langmead B, Salzberg SL (2015) HISAT: a fast spliced aligner with low memory requirements. Nature methods **12:** 357-360

Kimura M (1980) A simple method for estimating evolutionary rates of base substitutions through comparative studies of nucleotide sequences. Journal of Molecular Evolution **16:** 111-120

Leubner-Metzger G, Meins F (2001) Antisense-transformation reveals novel roles for class I beta-1,3-glucanase in tobacco seed after-ripening and photodormancy. Journal of experimental botany **362:** 1753-1759

Liang Z, Chen K, Li T, Zhang Y, Wang Y, Zhao Q, Liu J, Zhang H, Liu C, Ran Y, Gao C (2017) Efficient DNA-free genome editing of bread wheat using CRISPR/Cas9 ribonucleoprotein complexes. Nature communication **8:** 14261

Lin CS, Hsu CT, Yang LH, Lee LY, Fu JY, Cheng QW, Wu FH, Hsiao HC, Zhang Y, Zhang R, Chang WJ, Yu CT, Wang W, Liao LJ, Gelvin SB, Shih MC (2018) Application of protoplast technology to CRISPR/Cas9 mutagenesis: from single-cell mutation detection to mutant plant regeneration. Plant Biotechnology Journal **16:** 1295-1310

Li R, Sun S, Wang H, Wang K, Yu H, Zhou Z, Xin P, Chu J, Zhao T, Wang H, Li J, Cui X (2020) *FIS1* encodes a GA2-oxidase that regulates fruit firmness in tomato. Nature communication **11:** 5844

Liu B, Lu Y, Xin Z, Zhang Z (2009) Identification and antifungal assay of a wheat beta-1,3-glucanase. Biotechnology letters **31:** 1005-1010

Liu F, Cui X, Horner HT, Weiner H, Schnable PS (2001) Mitochondrial aldehyde dehydrogenase activity is required for male fertility in maize. The Plant Cell **13:** 1063-1078

Liu HZ, Zhang GS, Zhu WW, Ba QS, Niu N, Wang JW, Ma SC, Wang JS (2015) Relationship between male sterility and beta-1,3-glucanase activity and callose deposition-related gene expression in wheat (*Triticum aestivum* L.). Genetics and Molecular Research **14:** 574-584

Liu J, Zhang Y, Qin G, Tsuge T, Sakaguchi N, Luo G, Sun K, Shi D, Aki S, Zheng N, Aoyama T, Oka A, Yang W, Umeda M, Xie Q, Gu H, Qu LJ (2008) Targeted degradation of the cyclin-dependent kinase inhibitor ICK4/KRP6 by RING-type E3 ligases is essential for mitotic cell cycle progression during *Arabidopsis* gametogenesis. The Plant Cell **20:** 1538-54

Li N, Zhang DS, Liu HS, Yin CS, Li XX, Liang WQ, Yuan Z, Xu B, Chu HW, Wang J, Wen TQ, Huang H, Luo D, Ma H, Zhang DB (2006) The rice tapetum degeneration retardation gene is required for tapetum degradation and anther development. The Plant Cell **18:** 2999-3014

Li X, Li L, Yan J (2015) Dissecting meiotic recombination based on tetrad analysis by single-microspore sequencing in maize. Nature communication **6:** 6648

Lou Y, Xu XF, Zhu J, Gu JN, Blackmore S, Yang ZN (2014) The tapetal AHL family protein TEK determines nexine formation in the pollen wall. Nature communication **5:** 3855

Marchin M, Kelly PT, Fang J (2005) Tracker: continuous HMMER and BLAST searching. Bioinformatics **21:** 388-389

Marti E, Gisbert C, Bishop GJ, Dixon MS, Garcia-Martinez JL (2006) Genetic and physiological characterization of tomato cv. Micro-Tom. Journal of experimental botany **57:** 2037-2047

Martinelli F, Uratsu SL, Reagan RL, Chen Y, Tricoli D, Fiehn O, Rocke DM,

Gasser CS, Dandekar AM (2009) Gene regulation in parthenocarpic tomato fruit. Journal of experimental botany **60:** 3873-3890

Ma Y, Min L, Wang M, Wang C, Zhao Y, Li Y, Fang Q, Wu Y, Xie S, Ding Y, Su X, Hu Q, Zhang Q, Li X, Zhang X (2018) Disrupted genome methylation inresponse to high temperature has distinct effects on microspore abortion and anther indehiscence. The Plant Cell **30:** 1387-1403

Melonek J, Duarte J, Martin J, Beuf L, Murigneux A, Varenne P, Comadran J, Specel S, Levadoux S, Bernath-Levin K, Torney F, Pichon JP, Perez P, Small I (2021) The genetic basis of cytoplasmic male sterility and fertility restoration in wheat. Nature communication **2:** 1036.

Miller GL (1959) Use of DNS reagent for determination of reducing sugars. Analytical Chemistry **31:** 426–428.

Mistry J, Chuguransky S, Williams L, Qureshi M, Salazar GA, Sonnhammer E, Tosatto S, Paladin L, Raj S, Richardson LJ, Finn RD, Bateman A (2021) Pfam: The protein families database in 2021. Nucleic Acids Research **49:** D412-D419

Nishikawa S, Zinkl GM, Swanson RJ, Maruyama D, Preuss D (2005) Callose (beta-1,3 glucan) is essential for *Arabidopsis* pollen wall patterning, but not tube growth. BMC Plant Biology **5:** 22

Oh SA, Park HJ, Kim MH, Park SK (2021) Analysis of sticky generative cell mutants reveals that suppression of callose deposition in the generative cell is necessary for generative cell internalization and differentiation in *Arabidopsis*. The Plant Journal **106:** 228-244

Olimpieri I, Caccia R, Picarella ME, Pucci A, Santangelo E, Soressi GP, Mazzucato A (2011) Constitutive co-suppression of the GA 20-oxidase1 gene in tomato leads to severe defects in vegetative and reproductive development. Plant Science **180:** 496-503

Olsen OA (2001) Endosperm development: cellularization and cell fate specification. Annual Review of Plant Physiology and Plant Molecular Biology **52:** 233-267

Oide S, Bejai S, Staal J, Guan N, Kaliff M, Dixelius C (2013) A novel role of PR2 in abscisic acid (ABA) mediated, pathogen-induced callose deposition in *Arabidopsis thaliana*. New Phytologist **200:** 1187-1199

O'Lexy R, Kasai K, Clark N, Fujiwara T, Sozzani R, Gallagher KL (2018) Exposure to heavy metal stress triggers changes in plasmodesmatal permeability via deposition and breakdown of callose. Journal of experimental botany **69:** 3715-3728

Otegui M, Staehelin LA (2000) Syncytial-type cell plates: a novel kind of cell plate involved in endosperm cellularization of *Arabidopsis*. The Plant Cell **12:** 933-947

Parre E, Geitmann A (2005) More than a leak sealant. The mechanical properties of callose in pollen tubes. Plant Physiology **137:** 274-286

Pasoreck EK, Su J, Silverman IM, Gosai SJ, Gregory BD, Yuan JS, Daniell H (2016) Terpene metabolic engineering *via* nuclear or chloroplast genomes profoundly and globally impacts off-target pathways through metabolite signalling. Plant Biotechnology Journal **14:** 1862-1875

Pei YG, Tao QJ, Zheng XJ, Li Y, Sun XF, Li ZF, Qi XB, Xu J, Zhang M, Chen HB, Chang XL, Tang HM, Sui LY, Gong GS (2019) Phenotypic and genetic characterization of *Botrytis cinerea* population from kiwifruit in Sichuan province, China. Plant Diseases **103:** 748-758

Pervaiz T, Liu T, Fang X, Ren Y, Li X, Liu Z, Fiaz M, Fang J, Shangguan L (2021) Identification of *GH17* gene family in Vitis vinifera and expression analysis of *GH17* under various adversities. Physiology And Molecular Biology of Plants **27:** 1423-1436

Peterson R, Slovin JP, Chen C (2010) Simplified method for differential staining of

aborted and non-aborted pollen grains. International Journal of Plant Biology **1:** 66-69

Philippe S, Saulnier L, Guillon F (2006) Arabinoxylan and (1→3), (1→4)-β-glucan deposition in cell walls during wheat endosperm development. Planta **224:** 449-461

Qin Z, Yang D, You X, Liu Y, Hu S, Yan Q, Yang S, Jiang Z (2017) The recognition mechanism of triple-helical beta-1,3-glucan by a beta-1,3-glucanase. Chemical Communications **53:** 9368-9371

Rodriguez-Romero A, Hernandez-Santoyo A, Fuentes-Silva D, Palomares LA, Munoz-Cruz S, Yepez-Mulia L, Orozco-Martinez S (2014) Structural analysis of the endogenous glycoallergen Hev b 2 (endo-beta-1,3-glucanase) from Hevea brasiliensis and its recognition by human basophils. Acta Crystallographica. Section D: Biological Crystallography **70:** 329-341

Roggen HP, Stanley RG (1969) Cell-wall-hydrolysing enzymes in wall formation as measured by pollen-tube extension. Planta **84:** 295-303

Simpson C, Thomas C, Findlay K, Bayer E, Maule AJ (2009) An Arabidopsis GPI-anchor plasmodesmal neck protein with callose binding activity and potential to regulate cell-to-cell trafficking. The Plant Cell **21:** 581-594

Shikanai Y, Yoshida R, Hirano T, Enomoto Y, Li B, Asada M, Yamagami M, Yamaguchi K, Shigenobu S, Tabata R, Sawa S, Okada H, Ohya Y, Kamiya T, Fujiwara T (2020) Callose synthesis suppresses cell death induced by low-calcium conditions in leaves. Plant Physiology **182:** 2199-2212

Shinozaki Y, Nicolas P, Fernandez-Pozo N, Ma Q, Evanich DJ, Shi Y, Xu Y, Zheng Y, Snyder SI, Martin L, Ruiz-May E, Thannhauser TW, Chen K, Domozych DS, Catala C, Fei Z, Mueller LA, Giovannoni JJ, Rose J (2018) High-resolution spatiotemporal transcriptome mapping of tomato fruit development and ripening. Nature communication **9:** 364

Steiner-Lange S, Unte US, Eckstein L, Yang C, Wilson ZA, Schmelzer E, Dekker K, Saedler H (2003) Disruption of *Arabidopsis thaliana MYB26* results in male sterility due to non-dehiscent anthers. The Plant Journal **34:** 519-528

Stieglitz H (1977) Role of beta-1,3-glucanase in postmeiotic microspore release. Developmental Biology **57:** 87-97

Sun C, Fu D, Jin L, Chen M, Zheng X, Yu T (2018) Chitin isolated from yeast cell wall induces the resistance of tomato fruit to *Botrytis cinerea*. Carbohydr Polym **199:** 341-352

Suzuki T, Masaoka K, Nishi M, Nakamura K, Ishiguro S (2008) Identification of kaonashi mutants showing abnormal pollen exine structure in *Arabidopsis thaliana*. Plant And Cell Physiology **49:** 1465-77

Suzuki T, Narciso JO, Zeng W, Van De Meene A, Yasutomi M, Takemura S, Lampugnani ER, Doblin MS, Bacic A, Ishiguro S (2017) KNS4/UPEX1: a type II arabinogalactan β-(1,3)-galactosyltransferase required for pollen exine development. Plant Physiology **173:** 183-205.

Thomas BR, Romero GO, Nevins DJ, Rodriguez RL (2000) New perspectives on the endo-beta-glucanases of glycosyl hydrolase family 17. International Journal of Biological Macromolecules **27:** 139-144

Vogler F, Schmalzl C, Englhart M, Bircheneder M, Sprunck S (2014) Brassinosteroids promote *Arabidopsis* pollen germination and growth. Plant Reproduction **27:** 153-167

Wang B, Fang R, Zhang J, Han J, Chen F, He F, Liu Y, Chen L (2020) Rice *LecRK5* phosphorylates a UGPase to regulate callose biosynthesis during pollen development. Journal of experimental botany **71:** 4033-4041

Wang D, Kanyuka K, Papp-Rupar M (2022) Pectin: a critical component in cell-wall-mediated immunity. Trends in Plant Science **9:** S1360-1385(22)00262-X.

Wang D, Oses-Prieto JA, Li KH, Fernandes JF, Burlingame AL, Walbot V (2010)

The male sterile 8 mutation of maize disrupts the temporal progression of the transcriptome and results in the mis-regulation of metabolic functions. The Plant Journal **63:** 939-951

Wan L, Zha W, Cheng X, Liu C, Lv L, Liu C, Wang Z, Du B, Chen R, Zhu L, He G (2011) A rice beta-1,3-glucanase gene *Osg1* is required for callose degradation in pollen development. Planta **233:** 309-323

Wan X, Wu S, Li Z, Dong Z, An X, Ma B, Tian Y, Li J (2019) Maize genic male-sterility genes and their applications in hybrid breeding: progress and perspectives. Molecular Plant **12:** 321-342

Weier D, Thiel J, Kohl S, Tarkowská D, Strnad M, Schaarschmidt S, Weschke W, Weber H, Hause B (2014) Gibberellin-to-abscisic acid balances govern development and differentiation of the nucellar projection of barley grains. Journal of experimental botany **65:** 5291-5304

Wilson SM, Burton RA, Collins HM, Doblin MS, Pettolino FA, Shirley N, Fincher GB, Bacic A (2012) Pattern of deposition of cell wall polysaccharides and transcript abundance of related cell wall synthesis genes during differentiation in barley endosperm. Plant Physiology **159:** 655-670

Wu C, Yang Y, Su D, Yu C, Xian Z, Pan Z, Guan H, Hu G, Chen D, Li Z, Chen R, Hao Y (2022) The *SlHB8* acts as a negative regulator in tapetum development and pollen wall formation in Tomato. Horticulture Research **9:** c185

Wu SW, Kumar R, Iswanto A, Kim JY (2018) Callose balancing at plasmodesmata. Journal of experimental botany **69:** 5325-5339

Wu W, Li L, Zhao Y, Zhao Y, Jiang T, McCormick S, Zheng B (2021) Heterochromatic silencing is reinforced by *ARID1*-mediated small RNA movement in *Arabidopsis* pollen. New Phytologist **229:** 3269-3280

Wu X, Liu J, Li D, Liu CM (2016) Rice caryopsis development II: dynamic changes in the endosperm. Journal of Integrative Plant Biology **58:** 786-798

Yang L, Huang W, Xiong F, Xian Z, Su D, Ren M, Li Z (2017) Silencing of *SlPL*, which encodes a pectate lyase in tomato, confers enhanced fruit firmness, prolonged shelf-life and reduced susceptibility to grey mould. Plant Biotechnol J **15:** 1544-1555

Yang Z, Sun L, Zhang P, Zhang Y, Yu P, Liu L, Abbas A, Xiang X, Wu W, Zhan X, Cao L, Cheng S (2019) TDR INTERACTING PROTEIN 3, encoding a PHD-finger transcription factor, regulates Ubisch bodies and pollen wall formation in rice. The Plant Journal **99:** 844-861

Ye D, Rongpipi S, Kiemle SN, Barnes WJ, Chaves AM, Zhu C, Norman VA, Liebman-Pelaez A, Hexemer A, Toney MF, Roberts AW, Anderson CT, Cosgrove DJ, Gomez EW, Gomez ED (2020) Preferred crystallographic orientation of cellulose in plant primary cell walls. Nature communication **11:** 4720

Zhang D, Liu D, Lv X, Wang Y, Xun Z, Liu Z, Li F, Lu H (2014) The cysteine protease CEP1, a key executor involved in tapetal programmed cell death, regulates pollen development in *Arabidopsis*. The Plant Cell **26:** 2939-2961

Zhang D, Wu S, An X, Xie K, Dong Z, Zhou Y, Xu L, Fang W, Liu S, Liu S, Zhu T, Li J, Rao L, Zhao J, Wan X (2018) Construction of a multicontrol sterility system for a maize male-sterile line and hybrid seed production based on the *ZmMs7* gene encoding a PHD-finger transcription factor. Plant Biotechnology Journal **16:** 459-471

Zhang J, Wang Y, Naeem M, Zhu M, Li J, Yu X, Hu Z, Chen G (2019) An AGAMOUS MADS-box protein, SlMBP3, regulates the speed of placenta liquefaction and controls seed formation in tomato. Journal of experimental botany **70:** 909-924

Zhang Y, Butelli E, De Stefano R, Schoonbeek H, Magusin A, Pagliarani C, Wellner N, Hill L, Orzaez D, Granell A, Jones JDG, Martin C (2013) Anthocyanins double the shelf life of tomatoes by delaying overripening and

reducing susceptibility to gray mold. Current Biology **23:** 1094-1100

Zhu J, Lou Y, Shi QS, Zhang S, Zhou WT, Yang J, Zhang C, Yao XZ, Xu T, Liu JL, Zhou L, Hou JQ, Wang JQ, Wang S, Huang XH, Yang ZN (2020) Slowing development restores the fertility of thermo-sensitive male-sterile plant lines. Nature plants **6:** 360-367

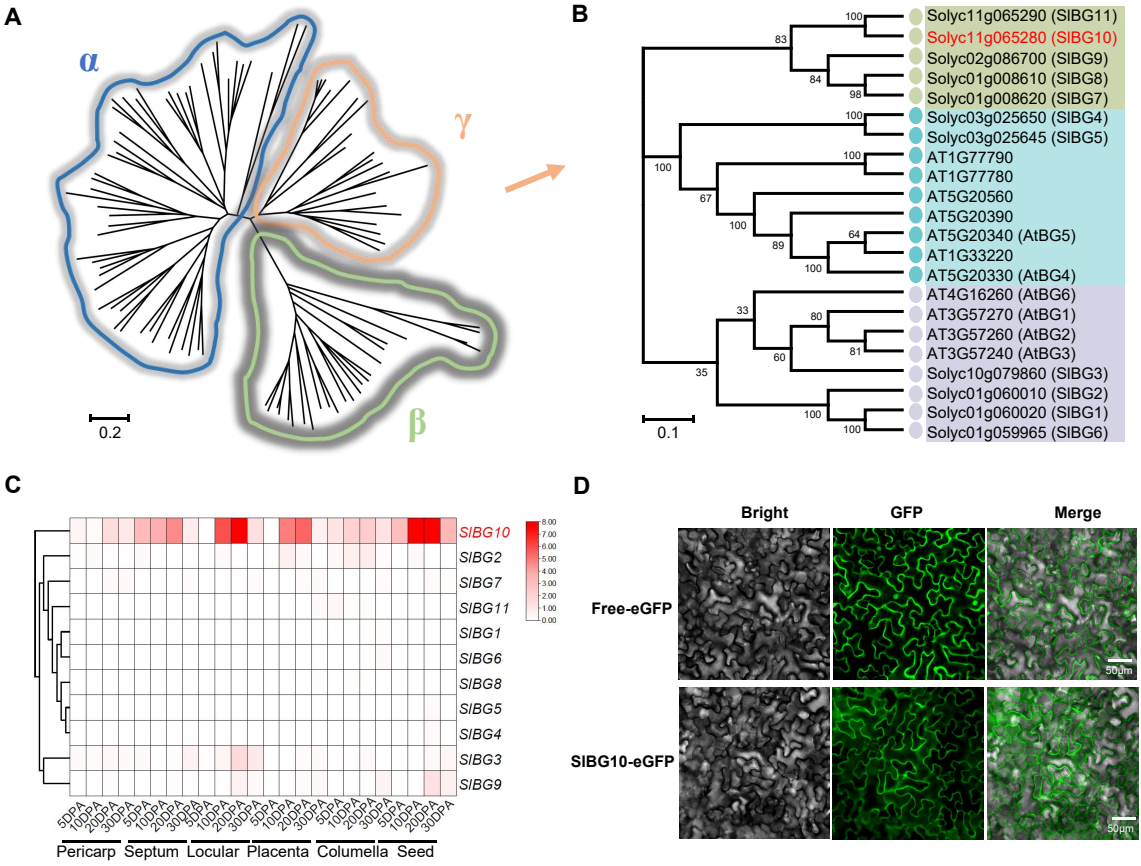

Figure 1. Identification of tomato GH17 genes. A, Phylogenetic tree of GH17 family proteins from tomato. All family members are divided into three clades, represented by different colors. B, Phylogenetic tree of β-1,3-glucanases of clade γ from *Arabidopsis thaliana* and *Solanum lycopersicum*. Proteins from different sub-clades are labeled with colored dots. C, Heatmap representation of the relative expression of clade γ genes in different tissues and developmental stages of tomato. DPA stands for days post-anthesis. D, Subcellular localization of SlBG10. *SlBG10* in-frame fused to green fluorescence protein (GFP) and free GFP were transiently expressed in *Nicotiana benthamiana* leaf epidermal cells.

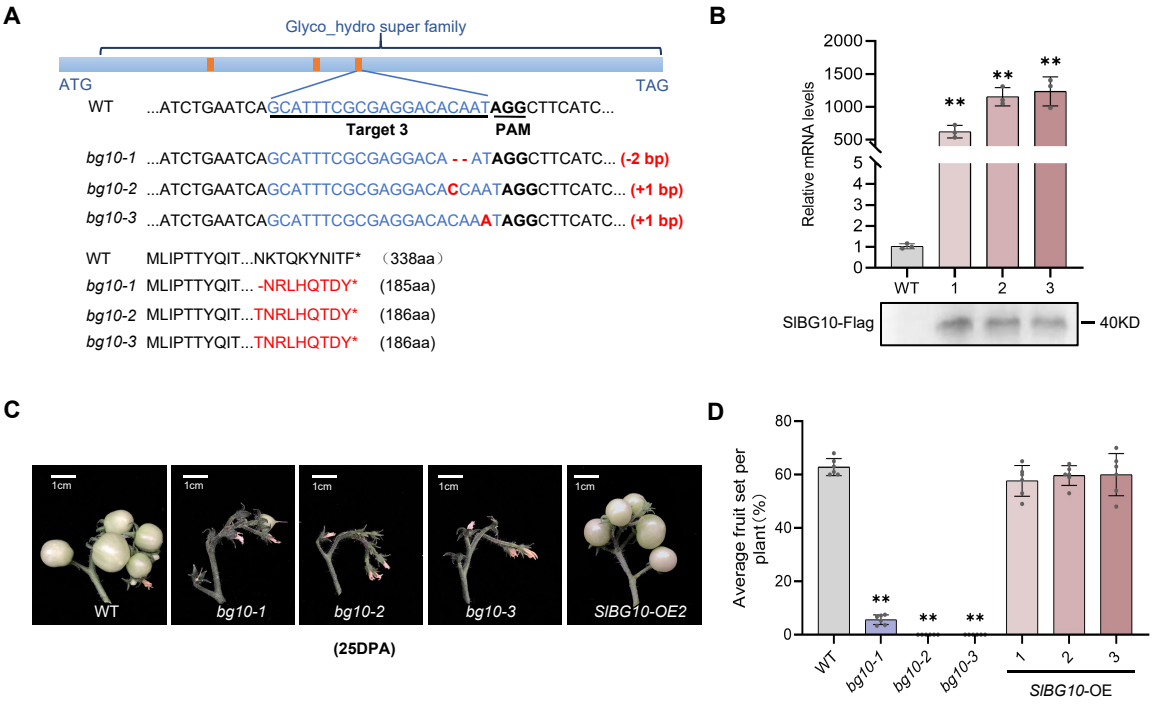

Figure 2. *SlBG10* is required for fruit setting in tomato. A, Outlines of *SlBG10*-knockout mutations generated by the CRISPR/Cas9 genome editing system. Three sequences targeting *SlBG10* were designed and three mutant-types of homozygous T1 lines *bg10-1*, *bg10-2* and *bg10-3* with premature translation stop codons were obtained. Orange boxes indicate the location of Targets 1-3. The sequences of Target 3 are highlighted blue. Domain of SlBG10, nucleotide deletion or insertion, as well as amino-acid (aa) sequences of WT and truncated SlBG10 are indicated. B, Relative *SlBG10* transcript levels in WT and *SlBG10* overexpression (*SlBG10*-OE) lines and Western blot analysis of SlBG10 protein levels in WT and *SlBG10*-OE lines. C and D, Fruit setting rate in WT, *bg10*, and *SlBG10*-OE lines. Photographs were taken at 25-DPA. Data are presented as means ± SD (n = 3 in B, n = 6 in D). Student's *t*-tests were performed and p values of *P < 0.05, **P < 0.01 indicate statistically significant when compared to WT.

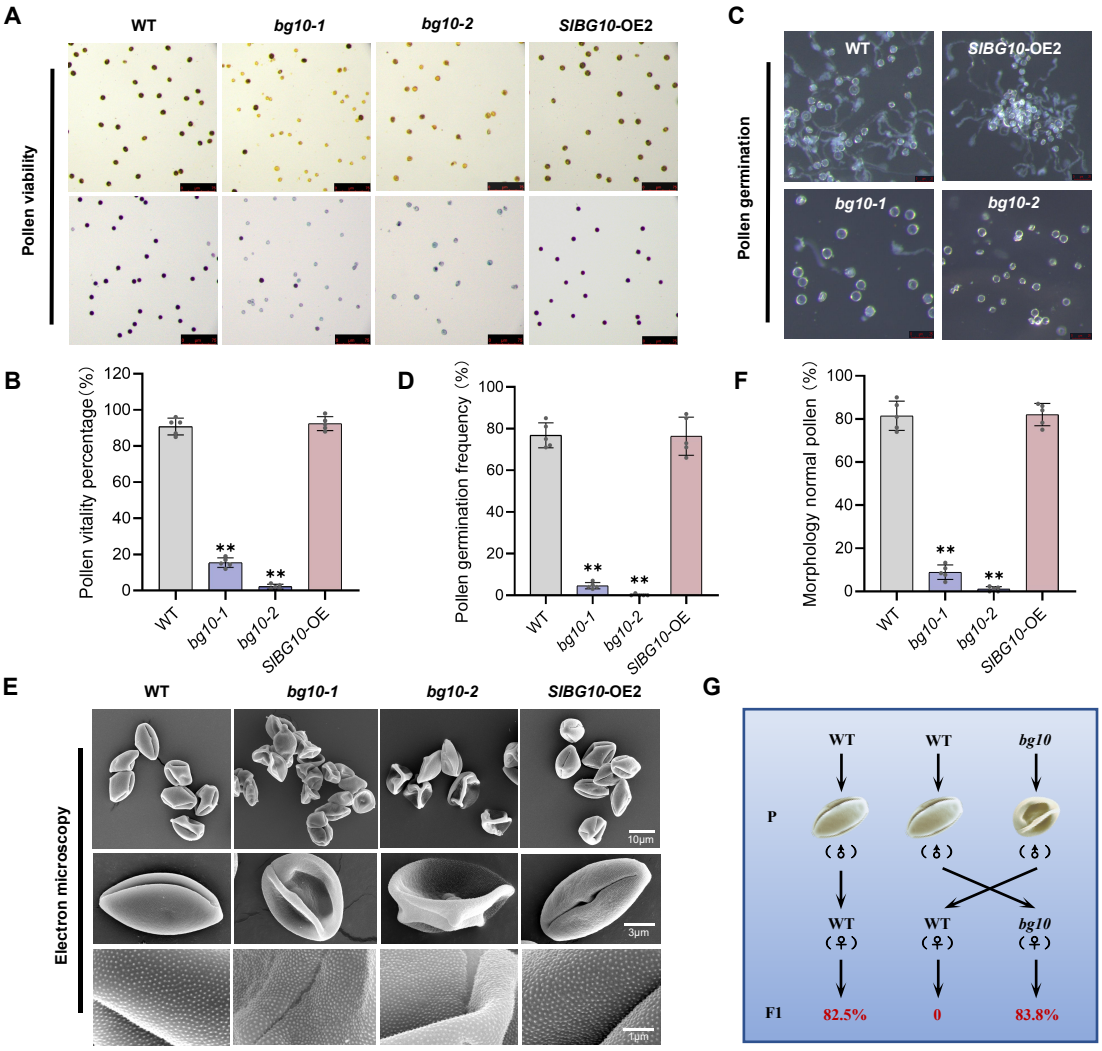

Figure 3. *SlBG10*-knockout *bg10* mutants exhibit reduction of pollen viability, germination rate and abnormal morphology compared to WT and *SlBG10*-OE lines. A, KI-I_2 (upper panel) and Alexander (lower panel) staining of mature pollens collected from WT, *bg10-1*, *bg10-2* and *SlBG10*-OE2 lines. Pollen grains that were viable stained black, while dead pollen grains stained yellow or light red by KI-I_2. Pollen grains that were viable stained dark blue or purple, while dead pollen grains were stained pale turquoise blue by Alexander. B, Percentage of viable pollen. C, *Ex-vitro* germination of mature pollens on pollen germination medium. D, Germination rate of mature pollens. E, SEM micrographs of pollen grains collected from WT, *bg10-1*, *bg10-2* and *SlBG10*-OE2 lines, respectively. F, Percentage of normal pollens. G, Reciprocal cross experiments between *bg10* and WT plants. Signs ♂ and ♀ represent male and female parent, respectively. Oval-shaped and shriveled pollens produced by WT plants or *bg10* lines are either viable or dead, respectively. Data are shown as means ± standard deviation (SD) (n = 5). Student's *t*-tests were performed and p values of *P < 0.05, **P < 0.01 indicate statistically significant when compared to WT.

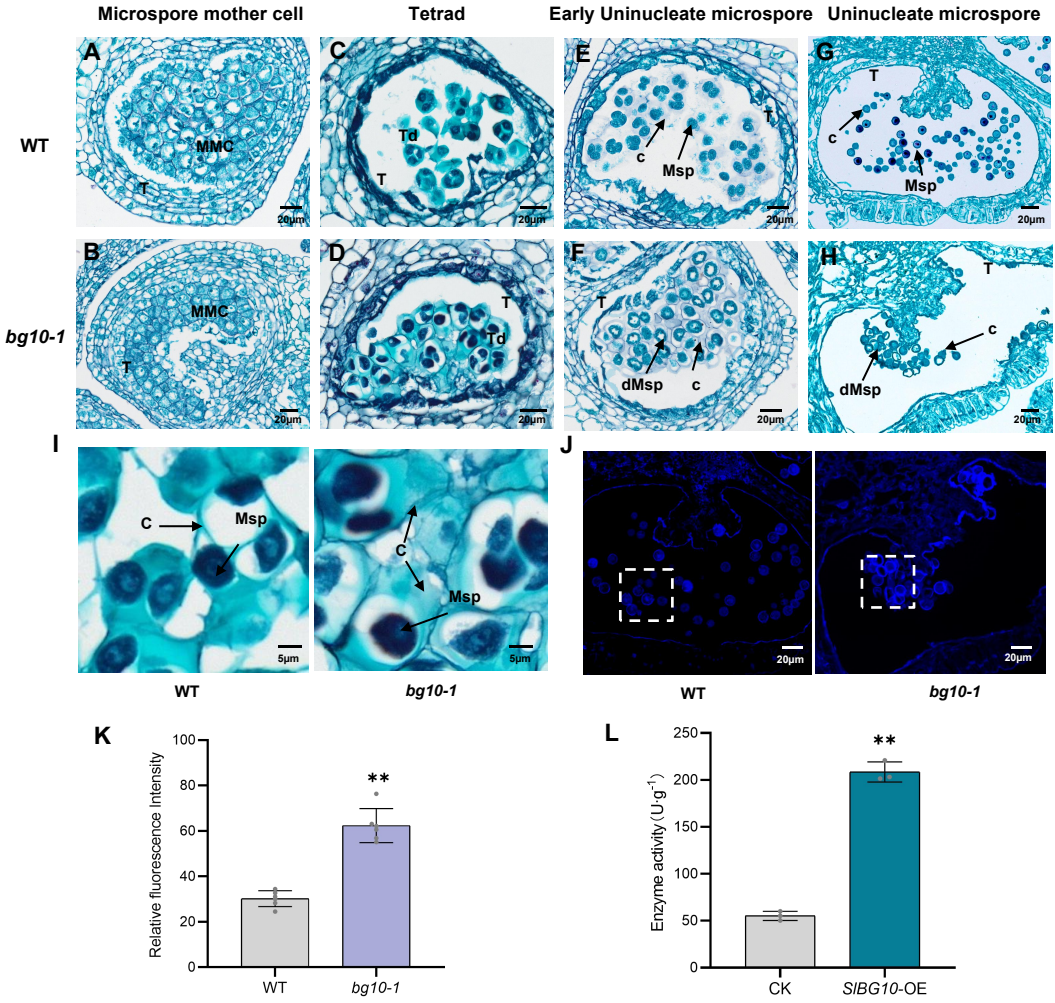

Figure 4. *SlBG10*-knockout *bg10* mutants display aberrant development of pollen and SlBG10 affects callose deposition around pollen grains. A-H, Histological observation of pollen development during microspore mother cell (MMC) to uninucleate microspore transition stage in WT and *bg10* lines. MMC, microspore mother cell; T, tapetum; Td, tetrad; Msp, microspore; dMsp, degenerated microspore; c, callose. I, Tetrads begin to degrade and microspores were released from callose wall in WT line, whilst callose deposition continued in the *bg10* mutant. J, Callose deposition was visible in aniline blue-stained anthers from WT and *bg10* lines under the fluorescence microscopy. The stronger fluorescence indicates the more callose deposits. K, Relative fluorescence Intensity of pollens from WT and *bg10* lines. L, Enzyme activity of SlBG10 to hydrolyze callose (β-1,3-glucan). Laminarin was used as substrate. Total proteins extracted from *E. coli* without or with IPTG induction were used as the negative control (CK) or SlBG10 enzymatic solution, respectively. Data are shown as means ± SD (n = 6 in D; n = 3 in E). Student's *t*-tests were performed and p values of *P < 0.05, **P < 0.01 indicate statistically significant when compared to CK.

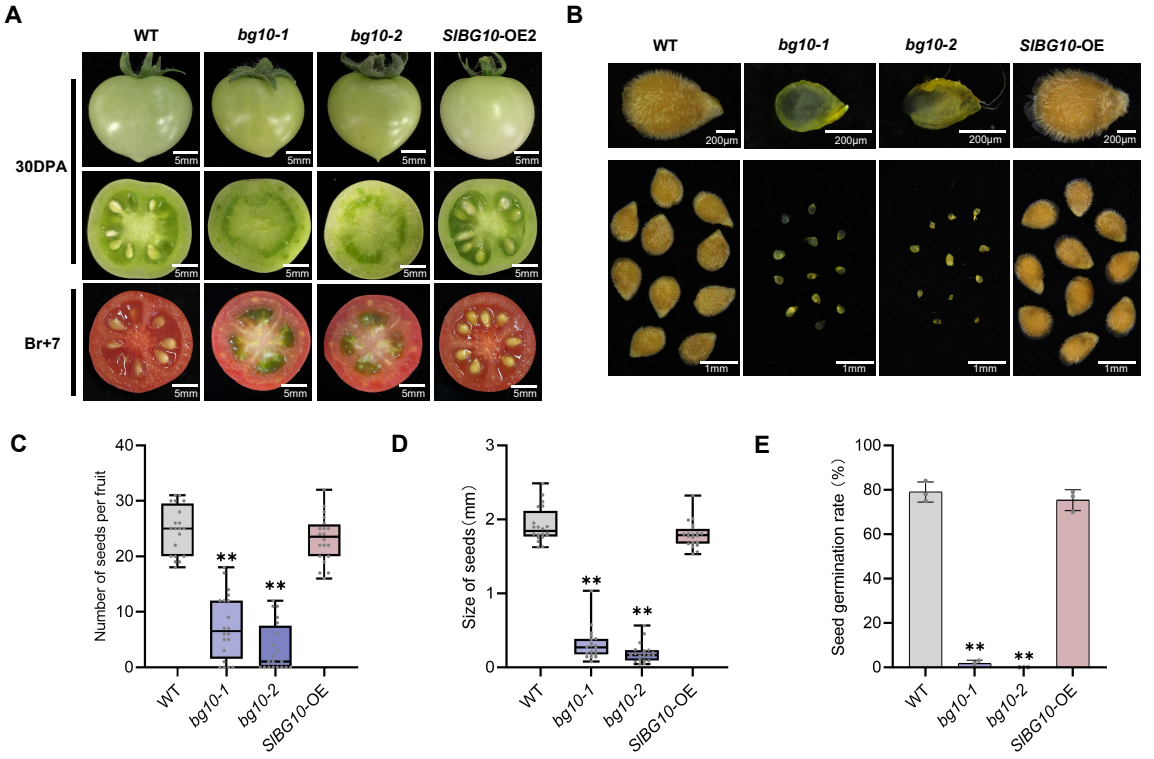

Figure 5. *SlBG10*-knockout *bg10* mutants exhibit seed abortion phenotype. A, Fruit sections of WT, *bg10-1*, *bg10-2* and *SlBG10*-OE2 lines. Fruits from *bg10-1*, *bg10-2* lines are seedless but mature seeds are produced in WT and *SlBG10*-OE line. B, Morphology of mature seeds from different lines. C, Number of seeds per fruit. D, Size of seeds. In the boxplots, the center line, box limits and whiskers denote the median, upper and lower quartiles and 1.5 × interquartile range, respectively. E, Seed germination rate. Data are shown as means ± SD (n = 20 in D and E; n = 3 in F), Student's *t*-tests were performed and p values of *P < 0.05, **P < 0.01 indicate statistically significant when compared to WT.

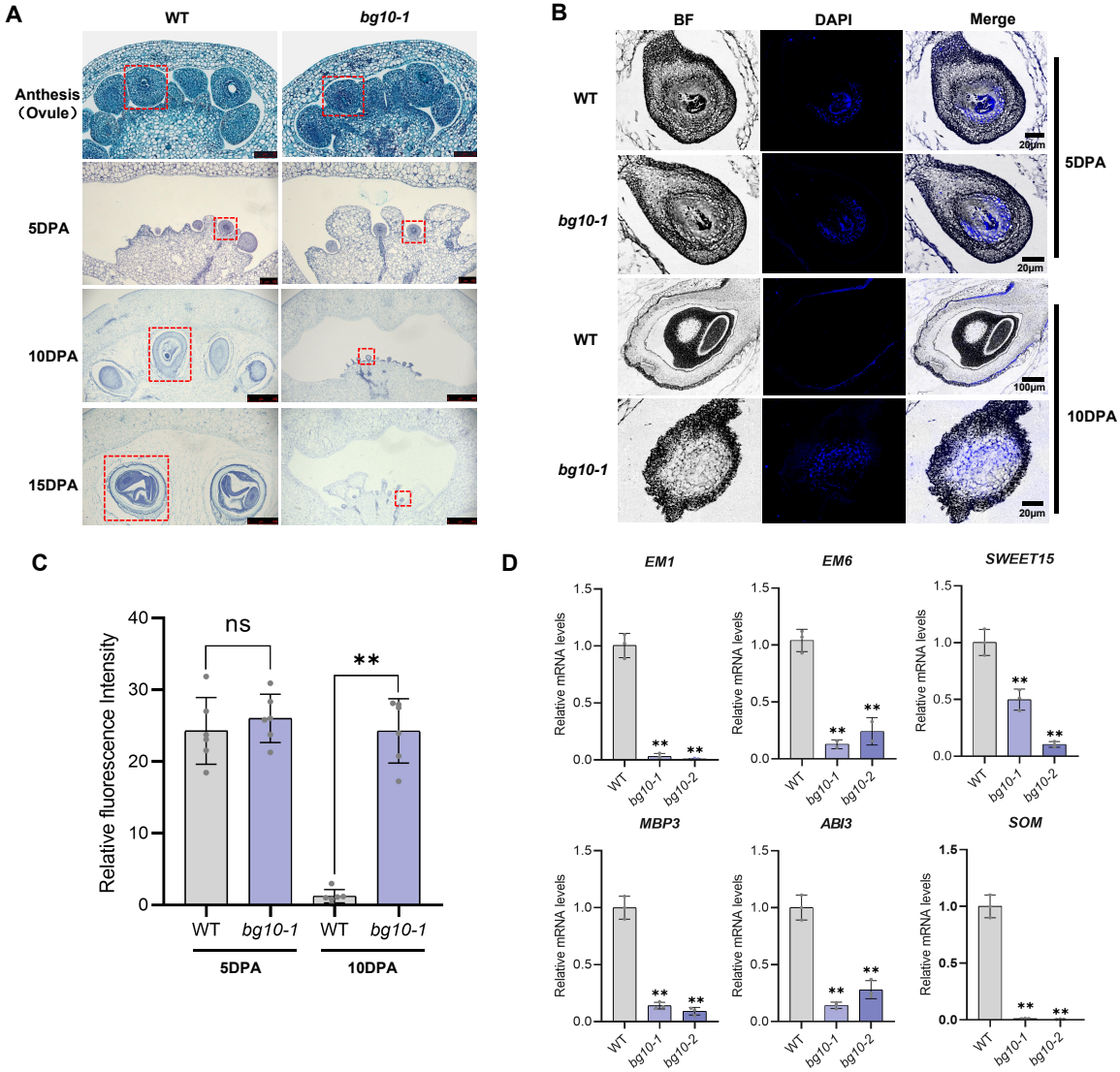

Figure 6. Abnormal callose deposition in the embryo results in early seed abortion. A, Transverse sections of fruits and seeds of WT and *bg10-1* line at anthesis (0-DPA), 5, 10 and 15 DPA. B, Callose deposition was visible in aniline blue-stained seeds from WT and bg10 lines under the fluorescence microscopy (BF, bight filed; DAPI, DAPI fluorescence; Merge, merge of DAPI and BF). C, Relative fluorescence intensity of seeds of WT and bg10 lines. D, Relative expression levels of seed development-related genes *EM1*, *EM6*, *SWEET15*, *MBP3*, *ABI3* and *SOM* in WT and *bg10* lines. Data are shown as means ± standard deviation (SD) (n = 6 in C; n = 3 in D), Student's *t*-tests were performed and p values of *P < 0.05, **P < 0.01 indicate statistically significant when compared to WT.

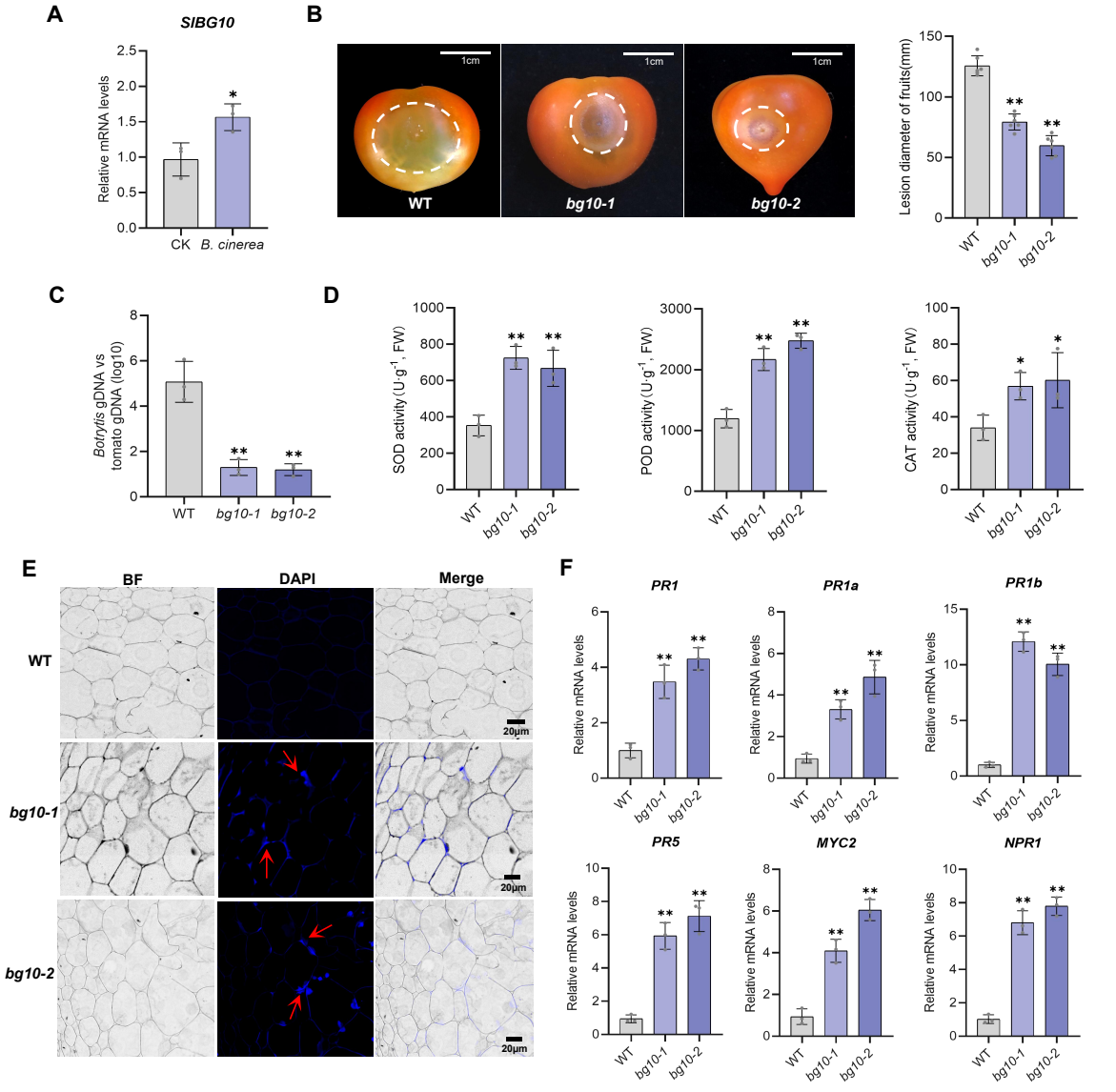

Figure 7. Disease resistance of *bg10* fruits. A, Induction of *SlBG10* expression by *Botrytis cinerea*. CK, blank PDA media. B, Disease symptoms on WT and *bg10* fruits at 48-hours after inoculation with mycelial plugs of *B. cinerea.* And the lesion diameter of tomato fruits. C, The ratio of *Botrytis* DNA to tomato DNA on WT and *bg10* fruits at 48-hours after inoculation with *B. cinerea*. D, Antioxidant enzymatic activities of SOD, POD and CAT after inoculation with *B. cinerea*. E, Callose deposition was visible in aniline blue-stained fruit pericarps from WT and *bg10* lines under the fluorescence microscopy. F, Relative expression levels of disease-resistance related genes *PR1*, *PR1a*, *PR1b*, *PR5*, *MYC2* and *NPR1* in WT and *bg10* lines. Data are presented as means ± SD (n = 3 in A, C, D and F; n = 6 in B). Student's *t*-tests were performed and p values of *P < 0.05, **P < 0.01 indicate statistically significant when compared to WT.

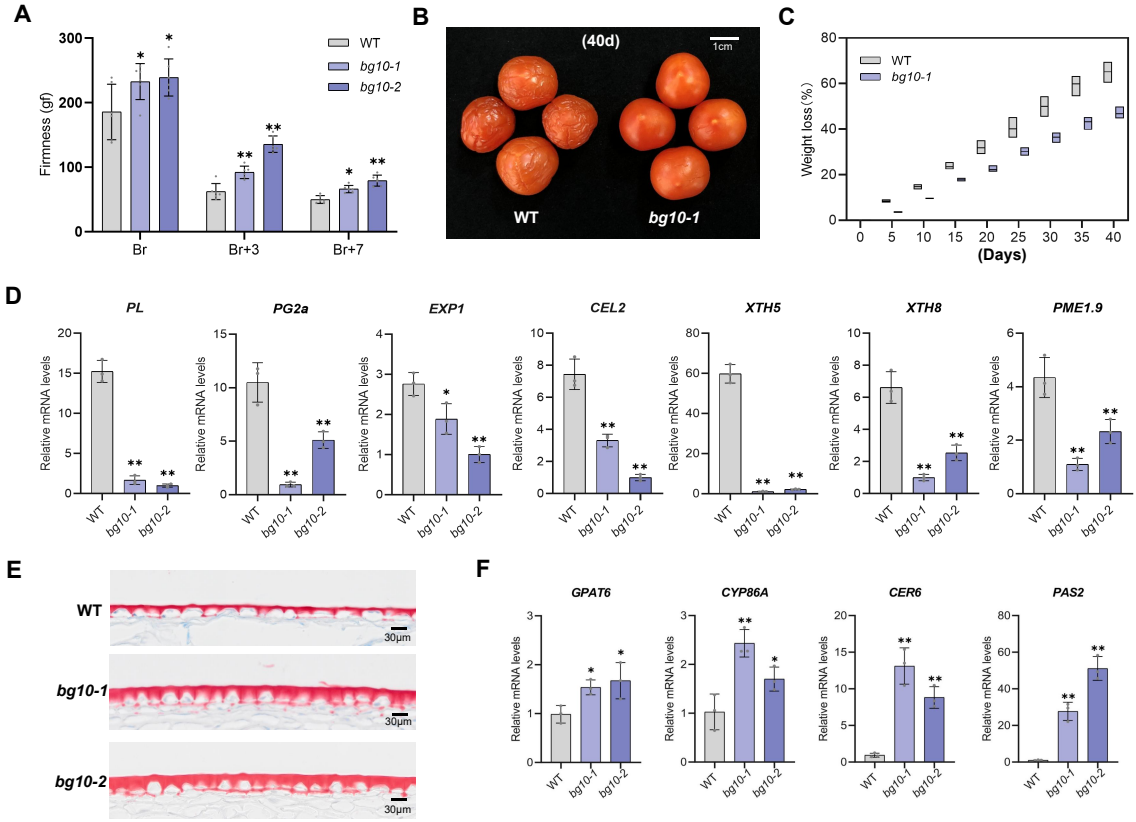

Figure 8. Knockout of *SlBG10* increases fruit firmness and extends shelf-life. A, Firmness of WT and *bg10* fruits at the Br (fruit at breaker), Br + 3 (3 days post-breaker) and Br + 7 (7 days post-breaker) stages. B, WT and *bg10-1* fruits harvested at BR + 7 stage and stored at 22℃. Photographs were taken at 40 days of storage. C, Lost fruit weight/fresh fruit weight ratio. In the boxplots, the center line, box limits and whiskers denote the median, upper and lower quartiles and 1.5 × interquartile range, respectively. D, Relative expression levels of fruit firmness-related genes *PL*, *EXP1*, *PG2a*, *CEL2*, *XTH5*, *XTH8* and *PME1.9* in WT and *bg10* lines. E, Cuticle thickness of WT and *bg10* fruits. F, Relative expression levels of cuticle synthesis-related genes *GPAT6*, *CYP86A*, *CER6* and *PAS2* in WT and *bg10* lines. Data are shown as means ± SD (n = 6 in A; n = 6 in C; n = 3 in E), Student's *t*-tests were performed and p values of *P < 0.05, **P < 0.01 indicate statistically significant when compared to WT.

Parsed Citations

Abad AR, Mehrtens BJ, Mackenzie SA (1995) Specific expression in reproductive tissues and fate of a mitochondrial sterility-associated protein in cytoplasmic male-sterile bean. The Plant Cell 7: 271-285
Google Scholar: Author Only Title Only Author and Title

Araki S, Le NT, Koizumi K, Villar-Briones A, Nonomura KI, Endo M, Inoue H, Saze H, Komiya R (2020) miR2118-dependent U-rich phasiRNA production in rice anther wall development. Nature communication 11: 3115
Google Scholar: Author Only Title Only Author and Title

Balasubramanian V, Vashisht D, Cletus J, Sakthivel N (2012) Plant β-1,3-glucanases: their biological functions and transgenic expression against phytopathogenic fungi. Biotechnology letters 34: 1983-1990
Google Scholar: Author Only Title Only Author and Title

Begcy K, Nosenko T, Zhou LZ, Fragner L, Weckwerth W, Dresselhaus T (2019) Male sterility in maize after transient heat stress during the tetrad stage of pollen development. Plant Physiology 181: 683-700
Google Scholar: Author Only Title Only Author and Title

Boavida LC, McCormick S (2007) Temperature as a determinant factor for increased and reproducible in vitro pollen germination in Arabidopsis thaliana. The Plant Journal 52: 570-582
Google Scholar: Author Only Title Only Author and Title

Borges A, Tsai SM, Caldas DG (2012) Validation of reference genes for RT-qPCR normalization in common bean during biotic and abiotic stresses. Plant Cell Reports 31: 827-838
Google Scholar: Author Only Title Only Author and Title

Brown RC, Lemmon BE, Stone BA, Olsen OA (1997) Cell wall (1→ 3)- and (1→ 3, 1→ 4)-β-glucans during early grain development in rice (Oryza sativa L.). Planta 202: 414-426
Google Scholar: Author Only Title Only Author and Title

Chang Z, Chen Z, Wang N, Xie G, Lu J, Yan W, Zhou J, Tang X, Deng XW (2016) Construction of a male sterility system for hybrid rice breeding and seed production using a nuclear male sterility gene. Proceedings of the National Academy of Sciences 113: 14145-14150
Google Scholar: Author Only Title Only Author and Title

Chen C, Chen H, Zhang Y, Thomas HR, Frank MH, He Y, Xia R (2020) TBtools: an integrative toolkit developed for interactive analyses of big biological data. Molecular Plant 13: 1194-1202
Google Scholar: Author Only Title Only Author and Title

Chen L, Yang D, Zhang Y, Wu L, Zhang Y, Ye L, Pan C, He Y, Huang L, Ruan YL, Lu G (2018) Evidence for a specific and critical role of mitogen-activated protein kinase 20 in uni-to-binucleate transition of microgametogenesis in tomato. New Phytologist 219: 176-194
Google Scholar: Author Only Title Only Author and Title

Chen S, Zhou Y, Chen Y, Gu J (2018) fastp: an ultra-fast all-in-one FASTQ preprocessor. Bioinformatics 34: i884-i890
Google Scholar: Author Only Title Only Author and Title

Chen R, Zhao X, Shao Z, Wei Z, Wang Y, Zhu L, Zhao J, Sun M, He R, He G (2007) Rice UDP-glucose pyrophosphorylase1 is essential for pollen callose deposition and its cosuppression results in a new type of thermosensitive genic male sterility. The Plant Cell 19: 847-61
Google Scholar: Author Only Title Only Author and Title

Conrath U, Klessig DF, Bachmair A (1998) Tobacco plants perturbed in the ubiquitin-dependent protein degradation system accumulate callose, salicylic acid, and pathogenesis-related protein 1. Plant Cell Reports 17: 876-880
Google Scholar: Author Only Title Only Author and Title

Cui Y, Li R, Li G, Zhang F, Zhu T, Zhang Q, Ali J, Li Z, Xu S (2020) Hybrid breeding of rice via genomic selection. Plant Biotechnology Journal 18: 57-67
Google Scholar: Author Only Title Only Author and Title

Deng H, Pirrello J, Chen Y, Li N, Zhu S, Chirinos X, Bouzayen M, Liu Y, Liu M (2018) A novel tomato F-box protein, SlEBF3, is involved in tuning ethylene signaling during plant development and climacteric fruit ripening. The Plant Journal 95: 648-658
Google Scholar: Author Only Title Only Author and Title

Deng H, Chen Y, Liu Z, Liu Z, Shu P, Wang R, Hao Y, Su D, Pirrello J, Liu Y, Li Z, Grierson D, Giovannoni JJ, Bouzayen M, Liu M (2022) SlERF. F12 modulates the transition to ripening in tomato fruit by recruiting the co-repressor TOPLESS and histone deacetylases to repress key ripening genes. The Plant Cell 34: 1250-1272
Google Scholar: Author Only Title Only Author and Title

De Jong M, Wolters-Arts M, Feron R, Mariani C, Vriezen WH (2009) The Solanum lycopersicum auxin response factor 7 (SlARF7)

regulates auxin signaling during tomato fruit set and development. The Plant Journal 57: 160-170
Google Scholar: Author Only Title Only Author and Title

De Storme N, Geelen D (2014) Callose homeostasis at plasmodesmata: molecular regulators and developmental relevance. Frontiers in plant science 5: 138
Google Scholar: Author Only Title Only Author and Title

De Storme N, De Schrijver J, Van Criekinge W, Wewer V, Dormann P, Geelen D (2013) GLUCAN SYNTHASE-LIKE8 and STEROL METHYLTRANSFERASE2 are required for ploidy consistency of the sexual reproduction system in Arabidopsis. The Plant Cell 25: 387-403
Google Scholar: Author Only Title Only Author and Title

Dong X, Hong Z, Sivaramakrishnan M, Mahfouz M, Verma DPS (2005) Callose synthase (CalS5) is required for exine formation during microgametogenesis and for pollen viability in Arabidopsis. The Plant Journal 42: 315-328
Google Scholar: Author Only Title Only Author and Title

Dou XY, Yang KZ, Ma ZX, Chen LQ, Zhang XQ, Bai JR, Ye D (2016). AtTMEM18 plays important roles in pollen tube and vegetative growth in Arabidopsis. Journal of Integrative Plant Biology 58: 679-92.
Google Scholar: Author Only Title Only Author and Title

Doxey AC, Yaish MW, Moffatt BA, Griffith M, McConkey BJ (2007) Functional divergence in the Arabidopsis beta-1,3-glucanase gene family inferred by phylogenetic reconstruction of expression states. Molecular Biology and Evolution 24: 1045-1055
Google Scholar: Author Only Title Only Author and Title

Ellinger D, Naumann M, Falter C, Zwikowics C, Jamrow T, Manisseri C, Somerville SC, Voigt CA (2013) Elevated early callose deposition results in complete penetration resistance to powdery mildew in Arabidopsis. Plant Physiology 161: 1433-1444
Google Scholar: Author Only Title Only Author and Title

Enns LC, Kanaoka MM, Torii KU, Comai L, Okada K, Cleland RE (2005) Two callose synthases, GSL1 and GSL5, play an essential and redundant role in plant and pollen development and in fertility. Plant Molecular Biology 58: 333-349
Google Scholar: Author Only Title Only Author and Title

Fan Y, Lin S, Li T, Shi F, Shan G, Zeng F (2022) The plasmodesmata-located beta-1,3-glucanase enzyme PdBG4 regulates trichomes growth in Arabidopsis thaliana. Cells 11: 2856
Google Scholar: Author Only Title Only Author and Title

Felsenstein J (1985) Confidence limits on phylogenies: an approach using the bootstrap. Evolution 39: 783-791
Google Scholar: Author Only Title Only Author and Title

Fernandez-San MA, Aranjuelo I, Douthe C, Nadal M, Ancin M, Larraya L, Farran I, Flexas J, Veramendi J (2018) Physiological performance of transplastomic tobacco plants overexpressing aquaporin AQP1 in chloroplast membranes. J Exp Bot 69: 3661-3673
Google Scholar: Author Only Title Only Author and Title

Gao J, Yan S, Yu H, Zhan M, Guan K, Wang Y, Yang Z (2019) Sweet sorghum (Sorghum bicolor L.) SbSTOP1 activates the transcription of a beta-1,3-glucanase gene to reduce callose deposition under Al toxicity: A novel pathway for Al tolerance in plants. Bioscience Biotechnology and Biochemistry 83: 446-455
Google Scholar: Author Only Title Only Author and Title

Garcia R, Botet J, Rodriguez-Pena JM, Bermejo C, Ribas JC, Revuelta JL, Nombela C, Arroyo J (2015) Genomic profiling of fungal cell wall-interfering compounds: identification of a common gene signature. BMC Genomics 16: 683
Google Scholar: Author Only Title Only Author and Title

Ge Z, Bergonci T, Zhao Y, Zou Y, Du S, Liu MC, Luo X, Ruan H, Garcia-Valencia LE, Zhong S, Hou S, Huang Q, Lai L, Moura DS, Gu H, Dong J, Wu HM, Dresselhaus T, Xiao J, Cheung AY, Qu LJ (2017) Arabidopsis pollen tube integrity and sperm release are regulated by RALF-mediated signaling. Science 358: 1596-1600.
Google Scholar: Author Only Title Only Author and Title

Guo Z, Slafer GA, Schnurbusch T (2016) Genotypic variation in spike fertility traits and ovary size as determinants of floret and grain survival rate in wheat. Journal of experimental botany 67: 4221-4230
Google Scholar: Author Only Title Only Author and Title

He Y, Yan L, Ge C, Yao XF, Han X, Wang R, Xiong L, Jiang L, Liu CM, Zhao Y (2019) PINOID is required for formation of the stigma and style in Rice. Plant Physiology 180: 926-936
Google Scholar: Author Only Title Only Author and Title

Hickerson N, Samuel MA (2022) Stylar steroids: brassinosteroids regulate pistil development and self-incompatibility in primula. Current Biology 32: R135-R137
Google Scholar: Author Only Title Only Author and Title

Hong Z, Delauney AJ, Verma DP (2001) A cell plate-specific callose synthase and its interaction with phragmoplastin. The Plant Cell 13: 755-768
Google Scholar: Author Only Title Only Author and Title

Huang B, Hu G, Wang K, Frasse P, Maza E, Djari A, Deng W, Pirrello J, Burlat V, Pons C, Granell A, Li Z, van der Rest B, Bouzayen M (2021) Interaction of two MADS-box genes leads to growth phenotype divergence of all-flesh type of tomatoes. Nature communication 12: 6892
Google Scholar: Author Only Title Only Author and Title

Ji K, Kai W, Zhao B, Sun Y, Yuan B, Dai S, Li Q, Chen P, Wang Y, Pei Y, Wang H, Guo Y, Leng P (2014) SlNCED1 and SlCYP707A2: key genes involved in ABA metabolism during tomato fruit ripening. Journal of experimental botany 65: 5243-5255
Google Scholar: Author Only Title Only Author and Title

Johns C, Lu M, Lyznik A, Mackenzie S (1992) A mitochondrial DNA sequence is associated with abnormal pollen development in cytoplasmic male sterile bean plants. The Plant Cell 4: 435-449
Google Scholar: Author Only Title Only Author and Title

Kim D, Langmead B, Salzberg SL (2015) HISAT: a fast spliced aligner with low memory requirements. Nature methods 12: 357-360
Google Scholar: Author Only Title Only Author and Title

Kimura M (1980) A simple method for estimating evolutionary rates of base substitutions through comparative studies of nucleotide sequences. Journal of Molecular Evolution 16: 111-120
Google Scholar: Author Only Title Only Author and Title

Leubner-Metzger G, Meins F (2001) Antisense-transformation reveals novel roles for class I beta-1,3-glucanase in tobacco seed after-ripening and photodormancy. Journal of experimental botany 362: 1753-1759
Google Scholar: Author Only Title Only Author and Title

Liang Z, Chen K, Li T, Zhang Y, Wang Y, Zhao Q, Liu J, Zhang H, Liu C, Ran Y, Gao C (2017) Efficient DNA-free genome editing of bread wheat using CRISPR/Cas9 ribonucleoprotein complexes. Nature communication 8: 14261
Google Scholar: Author Only Title Only Author and Title

Lin CS, Hsu CT, Yang LH, Lee LY, Fu JY, Cheng QW, Wu FH, Hsiao HC, Zhang Y, Zhang R, Chang WJ, Yu CT, Wang W, Liao LJ, Gelvin SB, Shih MC (2018) Application of protoplast technology to CRISPR/Cas9 mutagenesis: from single-cell mutation detection to mutant plant regeneration. Plant Biotechnology Journal 16: 1295-1310
Google Scholar: Author Only Title Only Author and Title

Li R, Sun S, Wang H, Wang K, Yu H, Zhou Z, Xin P, Chu J, Zhao T, Wang H, Li J, Cui X (2020) FIS1 encodes a GA2-oxidase that regulates fruit firmness in tomato. Nature communication 11: 5844
Google Scholar: Author Only Title Only Author and Title

Liu B, Lu Y, Xin Z, Zhang Z (2009) Identification and antifungal assay of a wheat beta-1,3-glucanase. Biotechnology letters 31: 1005-1010
Google Scholar: Author Only Title Only Author and Title

Liu F, Cui X, Horner HT, Weiner H, Schnable PS (2001) Mitochondrial aldehyde dehydrogenase activity is required for male fertility in maize. The Plant Cell 13: 1063-1078
Google Scholar: Author Only Title Only Author and Title

Liu HZ, Zhang GS, Zhu WW, Ba QS, Niu N, Wang JW, Ma SC, Wang JS (2015) Relationship between male sterility and beta-1,3-glucanase activity and callose deposition-related gene expression in wheat (Triticum aestivum L.). Genetics and Molecular Research 14: 574-584
Google Scholar: Author Only Title Only Author and Title

Liu J, Zhang Y, Qin G, Tsuge T, Sakaguchi N, Luo G, Sun K, Shi D, Aki S, Zheng N, Aoyama T, Oka A, Yang W, Umeda M, Xie Q, Gu H, Qu LJ (2008) Targeted degradation of the cyclin-dependent kinase inhibitor ICK4/KRP6 by RING-type E3 ligases is essential for mitotic cell cycle progression during Arabidopsis gametogenesis. The Plant Cell 20: 1538-54
Google Scholar: Author Only Title Only Author and Title

Li N, Zhang DS, Liu HS, Yin CS, Li XX, Liang WQ, Yuan Z, Xu B, Chu HW, Wang J, Wen TQ, Huang H, Luo D, Ma H, Zhang DB (2006) The rice tapetum degeneration retardation gene is required for tapetum degradation and anther development. The Plant Cell 18: 2999-3014
Google Scholar: Author Only Title Only Author and Title

Li X, Li L, Yan J (2015) Dissecting meiotic recombination based on tetrad analysis by single-microspore sequencing in maize. Nature communication 6: 6648
Google Scholar: Author Only Title Only Author and Title

Lou Y, Xu XF, Zhu J, Gu JN, Blackmore S, Yang ZN (2014) The tapetal AHL family protein TEK determines nexine formation in the pollen wall. Nature communication 5: 3855

Google Scholar: Author Only Title Only Author and Title

Marchin M, Kelly PT, Fang J (2005) Tracker: continuous HMMER and BLAST searching. Bioinformatics 21: 388-389
Google Scholar: Author Only Title Only Author and Title

Marti E, Gisbert C, Bishop GJ, Dixon MS, Garcia-Martinez JL (2006) Genetic and physiological characterization of tomato cv. Micro-Tom. Journal of experimental botany 57: 2037-2047
Google Scholar: Author Only Title Only Author and Title

Martinelli F, Uratsu SL, Reagan RL, Chen Y, Tricoli D, Fiehn O, Rocke DM, Gasser CS, Dandekar AM (2009) Gene regulation in parthenocarpic tomato fruit. Journal of experimental botany 60: 3873-3890
Google Scholar: Author Only Title Only Author and Title

Ma Y, Min L, Wang M, Wang C, Zhao Y, Li Y, Fang Q, Wu Y, Xie S, Ding Y, Su X, Hu Q, Zhang Q, Li X, Zhang X (2018) Disrupted genome methylation inresponse to high temperature has distinct effects on microspore abortion and anther indehiscence. The Plant Cell 30: 1387-1403
Google Scholar: Author Only Title Only Author and Title

Melonek J, Duarte J, Martin J, Beuf L, Murigneux A, Varenne P, Comadran J, Specel S, Levadoux S, Bernath-Levin K, Torney F, Pichon JP, Perez P, Small I (2021) The genetic basis of cytoplasmic male sterility and fertility restoration in wheat. Nature communication 2: 1036.
Google Scholar: Author Only Title Only Author and Title

Miller GL (1959) Use of DNS reagent for determination of reducing sugars. Analytical Chemistry 31: 426–428.
Google Scholar: Author Only Title Only Author and Title

Mistry J, Chuguransky S, Williams L, Qureshi M, Salazar GA, Sonnhammer E, Tosatto S, Paladin L, Raj S, Richardson LJ, Finn RD, Bateman A (2021) Pfam: The protein families database in 2021. Nucleic Acids Research 49: D412-D419
Google Scholar: Author Only Title Only Author and Title

Nishikawa S, Zinkl GM, Swanson RJ, Maruyama D, Preuss D (2005) Callose (beta-1,3 glucan) is essential for Arabidopsis pollen wall patterning, but not tube growth. BMC Plant Biology 5: 22
Google Scholar: Author Only Title Only Author and Title

Oh SA, Park HJ, Kim MH, Park SK (2021) Analysis of sticky generative cell mutants reveals that suppression of callose deposition in the generative cell is necessary for generative cell internalization and differentiation in Arabidopsis. The Plant Journal 106: 228-244
Google Scholar: Author Only Title Only Author and Title

Olimpieri I, Caccia R, Picarella ME, Pucci A, Santangelo E, Soressi GP, Mazzucato A (2011) Constitutive co-suppression of the GA 20-oxidase1 gene in tomato leads to severe defects in vegetative and reproductive development. Plant Science 180: 496-503
Google Scholar: Author Only Title Only Author and Title

Olsen OA (2001) Endosperm development: cellularization and cell fate specification. Annual Review of Plant Physiology and Plant Molecular Biology 52: 233-267
Google Scholar: Author Only Title Only Author and Title

Oide S, Bejai S, Staal J, Guan N, Kaliff M, Dixelius C (2013) A novel role of PR2 in abscisic acid (ABA) mediated, pathogen-induced callose deposition in Arabidopsis thaliana. New Phytologist 200: 1187-1199
Google Scholar: Author Only Title Only Author and Title

O'Lexy R, Kasai K, Clark N, Fujiwara T, Sozzani R, Gallagher KL (2018) Exposure to heavy metal stress triggers changes in plasmodesmatal permeability via deposition and breakdown of callose. Journal of experimental botany 69: 3715-3728
Google Scholar: Author Only Title Only Author and Title

Otegui M, Staehelin LA (2000) Syncytial-type cell plates: a novel kind of cell plate involved in endosperm cellularization of Arabidopsis. The Plant Cell 12: 933-947
Google Scholar: Author Only Title Only Author and Title

Parre E, Geitmann A (2005) More than a leak sealant. The mechanical properties of callose in pollen tubes. Plant Physiology 137: 274-286
Google Scholar: Author Only Title Only Author and Title

Pasoreck EK, Su J, Silverman IM, Gosai SJ, Gregory BD, Yuan JS, Daniell H (2016) Terpene metabolic engineering via nuclear or chloroplast genomes profoundly and globally impacts off-target pathways through metabolite signalling. Plant Biotechnology Journal 14: 1862-1875
Google Scholar: Author Only Title Only Author and Title

Pei YG, Tao QJ, Zheng XJ, Li Y, Sun XF, Li ZF, Qi XB, Xu J, Zhang M, Chen HB, Chang XL, Tang HM, Sui LY, Gong GS (2019) Phenotypic and genetic characterization of Botrytis cinerea population from kiwifruit in Sichuan province, China. Plant Diseases 103: 748-758

Google Scholar: Author Only Title Only Author and Title

Pervaiz T, Liu T, Fang X, Ren Y, Li X, Liu Z, Fiaz M, Fang J, Shangguan L (2021) Identification of GH17 gene family in Vitis vinifera and expression analysis of GH17 under various adversities. Physiology And Molecular Biology of Plants 27: 1423-1436
Google Scholar: Author Only Title Only Author and Title

Peterson R, Slovin JP, Chen C (2010) Simplified method for differential staining of aborted and non-aborted pollen grains. International Journal of Plant Biology 1: 66-69
Google Scholar: Author Only Title Only Author and Title

Philippe S, Saulnier L, Guillon F (2006) Arabinoxylan and (1→3), (1→4)-β-glucan deposition in cell walls during wheat endosperm development. Planta 224: 449-461
Google Scholar: Author Only Title Only Author and Title

Qin Z, Yang D, You X, Liu Y, Hu S, Yan Q, Yang S, Jiang Z (2017) The recognition mechanism of triple-helical beta-1,3-glucan by a beta-1,3-glucanase. Chemical Communications 53: 9368-9371
Google Scholar: Author Only Title Only Author and Title

Rodriguez-Romero A, Hernandez-Santoyo A, Fuentes-Silva D, Palomares LA, Munoz-Cruz S, Yepez-Mulia L, Orozco-Martinez S (2014) Structural analysis of the endogenous glycoallergen Hev b 2 (endo-beta-1,3-glucanase) from Hevea brasiliensis and its recognition by human basophils. Acta Crystallographica. Section D: Biological Crystallography 70: 329-341
Google Scholar: Author Only Title Only Author and Title

Roggen HP, Stanley RG (1969) Cell-wall-hydrolysing enzymes in wall formation as measured by pollen-tube extension. Planta 84: 295-303
Google Scholar: Author Only Title Only Author and Title

Simpson C, Thomas C, Findlay K, Bayer E, Maule AJ (2009) An Arabidopsis GPI-anchor plasmodesmal neck protein with callose binding activity and potential to regulate cell-to-cell trafficking. The Plant Cell 21: 581-594
Google Scholar: Author Only Title Only Author and Title

Shikanai Y, Yoshida R, Hirano T, Enomoto Y, Li B, Asada M, Yamagami M, Yamaguchi K, Shigenobu S, Tabata R, Sawa S, Okada H, Ohya Y, Kamiya T, Fujiwara T (2020) Callose synthesis suppresses cell death induced by low-calcium conditions in leaves. Plant Physiology 182: 2199-2212
Google Scholar: Author Only Title Only Author and Title

Shinozaki Y, Nicolas P, Fernandez-Pozo N, Ma Q, Evanich DJ, Shi Y, Xu Y, Zheng Y, Snyder SI, Martin L, Ruiz-May E, Thannhauser TW, Chen K, Domozych DS, Catala C, Fei Z, Mueller LA, Giovannoni JJ, Rose J (2018) High-resolution spatiotemporal transcriptome mapping of tomato fruit development and ripening. Nature communication 9: 364
Google Scholar: Author Only Title Only Author and Title

Steiner-Lange S, Unte US, Eckstein L, Yang C, Wilson ZA, Schmelzer E, Dekker K, Saedler H (2003) Disruption of Arabidopsis thaliana MYB26 results in male sterility due to non-dehiscent anthers. The Plant Journal 34: 519-528
Google Scholar: Author Only Title Only Author and Title

Stieglitz H (1977) Role of beta-1,3-glucanase in postmeiotic microspore release. Developmental Biology 57: 87-97
Google Scholar: Author Only Title Only Author and Title

Sun C, Fu D, Jin L, Chen M, Zheng X, Yu T (2018) Chitin isolated from yeast cell wall induces the resistance of tomato fruit to Botrytis cinerea. Carbohydr Polym 199: 341-352
Google Scholar: Author Only Title Only Author and Title

Suzuki T, Masaoka K, Nishi M, Nakamura K, Ishiguro S (2008) Identification of kaonashi mutants showing abnormal pollen exine structure in Arabidopsis thaliana. Plant And Cell Physiology 49: 1465-77
Google Scholar: Author Only Title Only Author and Title

Suzuki T, Narciso JO, Zeng W, Van De Meene A, Yasutomi M, Takemura S, Lampugnani ER, Doblin MS, Bacic A, Ishiguro S (2017) KNS4/UPEX1: a type II arabinogalactan β-(1,3)-galactosyltransferase required for pollen exine development. Plant Physiology 173: 183-205.
Google Scholar: Author Only Title Only Author and Title

Thomas BR, Romero GO, Nevins DJ, Rodriguez RL (2000) New perspectives on the endo-beta-glucanases of glycosyl hydrolase family 17. International Journal of Biological Macromolecules 27: 139-144
Google Scholar: Author Only Title Only Author and Title

Vogler F, Schmalzl C, Englhart M, Bircheneder M, Sprunck S (2014) Brassinosteroids promote Arabidopsis pollen germination and growth. Plant Reproduction 27: 153-167
Google Scholar: Author Only Title Only Author and Title

Wang B, Fang R, Zhang J, Han J, Chen F, He F, Liu Y, Chen L (2020) Rice LecRK5 phosphorylates a UGPase to regulate callose biosynthesis during pollen development. Journal of experimental botany 71: 4033-4041

Google Scholar: Author Only Title Only Author and Title

Wang D, Kanyuka K, Papp-Rupar M (2022) Pectin: a critical component in cell-wall-mediated immunity. Trends in Plant Science 9: S1360-1385(22)00262-X.
Google Scholar: Author Only Title Only Author and Title

Wang D, Oses-Prieto JA, Li KH, Fernandes JF, Burlingame AL, Walbot V (2010) The male sterile 8 mutation of maize disrupts the temporal progression of the transcriptome and results in the mis-regulation of metabolic functions. The Plant Journal 63: 939-951
Google Scholar: Author Only Title Only Author and Title

Wan L, Zha W, Cheng X, Liu C, Lv L, Liu C, Wang Z, Du B, Chen R, Zhu L, He G (2011) A rice beta-1,3-glucanase gene Osg1 is required for callose degradation in pollen development. Planta 233: 309-323
Google Scholar: Author Only Title Only Author and Title

Wan X, Wu S, Li Z, Dong Z, An X, Ma B, Tian Y, Li J (2019) Maize genic male-sterility genes and their applications in hybrid breeding: progress and perspectives. Molecular Plant 12: 321-342
Google Scholar: Author Only Title Only Author and Title

Weier D, Thiel J, Kohl S, Tarkowská D, Strnad M, Schaarschmidt S, Weschke W, Weber H, Hause B (2014) Gibberellin-to-abscisic acid balances govern development and differentiation of the nucellar projection of barley grains. Journal of experimental botany 65: 5291-5304
Google Scholar: Author Only Title Only Author and Title

Wilson SM, Burton RA, Collins HM, Doblin MS, Pettolino FA, Shirley N, Fincher GB, Bacic A (2012) Pattern of deposition of cell wall polysaccharides and transcript abundance of related cell wall synthesis genes during differentiation in barley endosperm. Plant Physiology 159: 655-670
Google Scholar: Author Only Title Only Author and Title

Wu C, Yang Y, Su D, Yu C, Xian Z, Pan Z, Guan H, Hu G, Chen D, Li Z, Chen R, Hao Y (2022) The SlHB8 acts as a negative regulator in tapetum development and pollen wall formation in Tomato. Horticulture Research 9: c185
Google Scholar: Author Only Title Only Author and Title

Wu SW, Kumar R, Iswanto A, Kim JY (2018) Callose balancing at plasmodesmata. Journal of experimental botany 69: 5325-5339
Google Scholar: Author Only Title Only Author and Title

Wu W, Li L, Zhao Y, Zhao Y, Jiang T, McCormick S, Zheng B (2021) Heterochromatic silencing is reinforced by ARID1-mediated small RNA movement in Arabidopsis pollen. New Phytologist 229: 3269-3280
Google Scholar: Author Only Title Only Author and Title

Wu X, Liu J, Li D, Liu CM (2016) Rice caryopsis development II: dynamic changes in the endosperm. Journal of Integrative Plant Biology 58: 786-798
Google Scholar: Author Only Title Only Author and Title

Yang L, Huang W, Xiong F, Xian Z, Su D, Ren M, Li Z (2017) Silencing of SlPL, which encodes a pectate lyase in tomato, confers enhanced fruit firmness, prolonged shelf-life and reduced susceptibility to grey mould. Plant Biotechnol J 15: 1544-1555
Google Scholar: Author Only Title Only Author and Title

Yang Z, Sun L, Zhang P, Zhang Y, Yu P, Liu L, Abbas A, Xiang X, Wu W, Zhan X, Cao L, Cheng S (2019) TDR INTERACTING PROTEIN 3, encoding a PHD-finger transcription factor, regulates Ubisch bodies and pollen wall formation in rice. The Plant Journal 99: 844-861
Google Scholar: Author Only Title Only Author and Title

Ye D, Rongpipi S, Kiemle SN, Barnes WJ, Chaves AM, Zhu C, Norman VA, Liebman-Pelaez A, Hexemer A, Toney MF, Roberts AW, Anderson CT, Cosgrove DJ, Gomez EW, Gomez ED (2020) Preferred crystallographic orientation of cellulose in plant primary cell walls. Nature communication 11: 4720
Google Scholar: Author Only Title Only Author and Title

Zhang D, Liu D, Lv X, Wang Y, Xun Z, Liu Z, Li F, Lu H (2014) The cysteine protease CEP1, a key executor involved in tapetal programmed cell death, regulates pollen development in Arabidopsis. The Plant Cell 26: 2939-2961
Google Scholar: Author Only Title Only Author and Title

Zhang D, Wu S, An X, Xie K, Dong Z, Zhou Y, Xu L, Fang W, Liu S, Liu S, Zhu T, Li J, Rao L, Zhao J, Wan X (2018) Construction of a multicontrol sterility system for a maize male-sterile line and hybrid seed production based on the ZmMs7 gene encoding a PHD-finger transcription factor. Plant Biotechnology Journal 16: 459-471
Google Scholar: Author Only Title Only Author and Title

Zhang J, Wang Y, Naeem M, Zhu M, Li J, Yu X, Hu Z, Chen G (2019) An AGAMOUS MADS-box protein, SlMBP3, regulates the speed of placenta liquefaction and controls seed formation in tomato. Journal of experimental botany 70: 909-924
Google Scholar: Author Only Title Only Author and Title

Zhang Y, Butelli E, De Stefano R, Schoonbeek H, Magusin A, Pagliarani C, Wellner N, Hill L, Orzaez D, Granell A, Jones JDG,

Martin C (2013) Anthocyanins double the shelf life of tomatoes by delaying overripening and reducing susceptibility to gray mold. Current Biology 23: 1094-1100
Google Scholar: Author Only Title Only Author and Title

Zhu J, Lou Y, Shi QS, Zhang S, Zhou WT, Yang J, Zhang C, Yao XZ, Xu T, Liu JL, Zhou L, Hou JQ, Wang JQ, Wang S, Huang XH, Yang ZN (2020) Slowing development restores the fertility of thermo-sensitive male-sterile plant lines. Nature plants 6: 360-367
Google Scholar: Author Only Title Only Author and Title